JIMMA UNIVERSITY

COLLEGE OF SOCIAL SCIENCES AND HUMANITIES

DEPARTMENT OF GEOGRAPHY AND ENVIRONMENTAL STUDIES

LAND SURFACE TEMPERATURE DETECTION IN RELATION TO FOREST COVER CHANGE: THE CASE OF JIMMA CITY AND IT'S SURROUNDINGS, JIMMA ZONE, SOUTHWEST, ETHIOPIA

BY

NIGUS TEKLESELASSIE

A THESIS SUBMITTED TO JIMMA UNIVERSITY, COLLEGE OF SOCIAL SCIENCES AND HUMANITIES, DEPARTMENT OF GEOGRAPHY AND ENVIRONMENTAL STUDIES FOR SPATIAL FULFILMENNT OF THE REQUIRMENTS FOR THE MASTER'S DEGREE OF SCIENCE IN GEOGRAPHIC INFORMATION SYSTEM AND REMOTE SENSING.

AUGUST, 2021

JIMMA, ETHIOPIA

LAND SURFACE TEMPERATURE DETECTION IN RELATION TO FOREST COVER CHANGE: IN JIMMA CITY AND IT'S SURROUNDINGS, SOUTHWESTERN ETHIOPIA

By

NigusTekleselassie

Submitted to the Department of Geography and Environmental Studies, Jimma University College of Social Sciences and Humanities, in Partial Fulfillment of the Requirements for the Degree of Masters of Science in Geographic Information Systems and Remote Sensing.

Major advisor: Girma Alemu (Ph.D. Scholar)

Co-advisor: Solomon Cheru (MSc)

August, 2021

Jimma, Ethiopia

ACKNOWLEDGEMENTS

I would like to extend my deepest gratitude, first and foremost, to God, who creates this world in his word and help us in all aspects of our life. This thesis appears in its current form due to the assistance and guidance of several people. I would therefore like to offer my sincere thanks to all of them. I would like to express my sincere thanks to my major advisor Mr. Girma Alemu for his regular support, gentleness, keen support, and close follow-up while I am conducting this research from the very beginning of the development of the research proposal to the accomplishment of the report. I would also like to acknowledge my co-advisor Mr. Solomon Cheru, for his critical comments and ideas with inclusive support in the structure and arrangement of the thesis work at various levels. Special thanks to all my friends who helping me and guiding me by spending their expensive time.

Table of Contents

List of Tables

List of Figures

ABBREVIATIONS

CSA	Central Statistical Agency
DIP	Digital Image Processing
DN	Digital Number
ENVI	Environment for Visualizing Images
ERDAS	Earth Resources Data Analysis System
ETM+	Enhanced Thematic Mapper Plus
FAO	Food and Agriculture Organization
FV	Fractional vegetation
GHG	Greenhouse Gasses
GPS	Global Positioning System
IPCC	Intergovernmental Panel on Climate Change
KII	Key Informant Interview
LST	Land Surface Temperature
LULC	Land-use and land-cover
NASA	National Aeronautics and Space Administration
NDBI	Normalized Difference Built-up Index
NDVI	Normalized Difference Vegetation Index
OLI	Operational Land Imagery
SPSS	Statistical Package for the Social Sciences
TIR	Thermal Infrared
TIRS	Thermal Infrared Sensor
TM	Thematic Mapper
UNEP	United Nation Environmental Program
USGS	United States Geological Survey

ABSTRACT

Unmanaged land use and land cover change is one of the main environmental problems and challenges, which strongly influence the process of urbanization and agricultural development. This change in land cover is responsible for increasing the land surface temperature. The present study assesses the effect of land use land cover (LULC) change on land surface temperature in Jimma city and its surrounding. LULC, Normalized Difference Vegetation Index (NDVI), Normalized Difference Built-up Index (NDBI), and Land Surface Temperature (LST) were extracted from Landsat 5 TM (1987), Landsat 7 ETM^{+} (2003), and Landsat 8 OLI/TIRS (2019) using digital image processing techniques. Change detaction techniques were used to analyze LULC changes from 1987 to 2019. This study also analyzes the effect of NDVI and NDBI on LST between 1987 and 2019 with 368 sample points selected by stratified random sampling and using a multiple linear regression model. The result showed that during the study period 1987-2019, agricultural land was the dominant land use which covered 54% of the study area. Settlement and agricultural land areas increased from 4.4% and 54.58% in 1987 to 12.27% and 62.40% in 2019 with the mean increase in land surface temperature from 20.53°C and 19.59°C to 33.60°C and 25.82°C, respectively. Forest cover, shrubland, waterbody, and wetland show decreasing trend. Correlation results of LST and NDBI have shown a strong positive relationship i.e. R^2 = 0.754 in 1987, 0.754 in 2003, and 0.739 in 2019, whereas strong negative correlations were found between LST and NDVI i.e. R^2 = 0.701, 0.737, and 0.746 in each year. The relationship between NDVI & NDBI was also developed and is showing a strong negative correlation i.e. R^2 = 0.739, 0.860, and 0.801. Hence, it was recommended that to reduce the land surface temperature, sustainable land use planning strategies that include increasing the vegetated areas and embracing other green initiatives such as the afforestation program should be adopted.

***Keywords**: Land Surface Temperature, LULC, NDVI, NDBI, Multiple linear regression*

CHAPTE ONE

1. INTRODUCTION

1.1. Background of the study

The surface of the earth has been modified for thousands of years due to human-induced activities (Veldkamp & Lambin, 2001). These environmental changes are intensified by high population pressure, migration, and accelerated socio-economic activities (Zengin, *et al.,* 2018). The changes have been found in various spatial scales from local to global levels (Mahmood *et al.,* 2010). Large-scale human activities like agriculture and settlement expansion are continuously decreasing the vegetation cover of the earth's surface. Consequently, the concentration of carbon dioxide is increasing in the atmosphere which in turn affecting the surface energy budget thereby producing changes in local, regional, and global climate (Lilly R. & Devadas, 2009).

Population increase leads to a quick expansion of urban growth, causing changes in land use land cover (LULC) in many urban areas (Coskun *et al.,* 2008). Urbanization has been increased from time to time with the increase of population number and rural-urban migration, particularly in developing countries. Developing countries especially Africa and Asia contribute more to this rapid increase of urbanization (UN-Habitat, 2010). Mainly, from 2010-2015 urbanization in Africa is continuously increasing and predicted to be 56% with an annual increment of 1.1%. In the same way, Ethiopia is one of the nations in Africa where urban dwellers have been increasing from 19% in 2014 and are expected to be 38% in 2050. According to the UN (2014) report, the urban growth rate of Ethiopia between 2010-2015 was 2.3%.

According to Sahoo (2013), the rapid urbanization process brought about many eco-environmental problems, such as the drastic change of land use and the development of land surface temperature (LST). Urban development coupled with unsustainable land management practices has a great impact on the local climate of a city. The abrupt land cover changes modify the amount of absorption of solar radiation, evaporation rates, thermal storage of surfaces, and wind turbulence (Polydoros, *et al.,* 2018). The exploitation

of the natural environment by a human being through urban development and expansion has a major impact on the urban microclimate at the local and global climate on a wider scale. One major phenomenon that arises as a result of this exploitation is the increase in land surface temperature (Igun & Williams, 2018).

Changes in LULC have a substantial impact on urban surface energy budgets (Alshaikh, 2015). It also resulted in a shift in urban form and microclimate (Alqurashi & Kumar, 2013). Due to the transition of LULC classes into non-evaporating surfaces, the surface temperature has risen (Sahana *et al.,* 2016).

The necessity to adequately analyze the impact of LULC modifications on the overall increase in the LST is becoming more pressing. Because different LULC surfaces or kinds release and absorb energy radiation in different ways, they have been studied to estimate LST (Pongratz, *et al.,* 2010). Estimating the cross-sectional relationship between LST and LULC types has also aided researchers in looking at the influence of land cover changes on LST through time (Liu & Zhang, 2011). Several studies have been conducted in cities to study the variability of the LST as a result of shifting urban land cover types. Hu & Jia (2010) found that between 1990 and 2007, a decadal decline in vegetation owing to changes in urban land cover in Guangzhou, southern China, resulted in an overall increase of 2.48 °C in LST. Due to the alteration in plant cover caused by urban expansion, a comparison study of Mumbai and Delhi found that the intensity of the UHI was higher in Mumbai than in Delhi (Grover & Singh, 2015). The land surface temperature in Bahir Dar was investigated using the normalized difference vegetation index (NDVI) and LULC measures. It was reported that the conversion of LULC to urban landscap increased LST. Accordingly, the maximum temperature in 1987 was 34.93 °C and in 2017 it reached 43.01 °C. This shows an 8.08°C increment in LST (Balew, 2018). When moving from a highly vegetated to a sparsely vegetated region, (Amiri *et al.,* 2009) found that the surface temperature values fluctuate. In most metropolitan locations, it has been observed that tree cover or vegetation is inversely related to the LST (Raynolds et al., 2008; Weng & Lu, 2008; Weng et al., 2004). However, vegetation has long been thought to play an important role in reducing the impact of urban heating in metropolitan settings (Zhibin et al., 2015; Chen et al., 2013; Onishi et al., 2010; Ali-Toudert & Mayer, 2007). However, properly

identifying hot spot areas inside existing urban areas, as well as the integration of vegetated areas into existing built-up areas, has been a difficulty (Rotem-Mindali *et al.,* 2015).

As a result, it is critical to track the trajectory of LULC change and its dynamism in order to maintain global climate change (Aadil et al., 2014). As a result, landscape analysis is an effective method for tracking different LULC patterns and their variations (Arvor et al., 2014). Analyzing the impacts of LULC changes on the Earth's surface, such as land surface temperature (LST) changes and distributions, is also critical.

1.2. Statement of the problem

One of the most important factors that are responsible for the increments of land surface temperature is Forest cover change (Gao & Liu, 2012). In recent times, global warming and environmental change-related problems are the major issues for both developed and developing countries (Musa *et al.,* 2018). Thus environmental problems are mainly attributed to the expansion of urban and increasing needs for land for settlement and industrial activities. Practices such as deforestation and unplanned land use for settlement and other activity leads our environment to the warmer temperature.

It is observed that the Land Surface Temperature (LST) of Jimma City and its surrounding has been increasing from season to season. According to National Meteorological Agency/Western Oromia Service Center (2019), the average temperature of the study area in 1987 and 2019 was 22.47 ^{0}C and 24.05 ^{0}C respectively. This indicates that average temperature has risen by 1.58°C over 32 years, but the dynamics are difficult to grasp without understanding of the LULC shift that causes LST change.

As a result, considerably greater surface temperatures in the city increase the need for air conditioning and water and power usage, as well as changing precipitation patterns, which might affect biotic ecosystems. The comfort of city inhabitants may be harmed by excessive heat, which can lead to increased health risks (Claus & Mushtaq, 2011). The air temperature of the atmospheric boundary layer is also influenced by land surface temperature, which is an important factor in the town's surface energy balance. As a result, changes in urban LST can have a big impact on Jimma city's weather and climate (Claus & Mushtaq, 2011). This is due to the fact that the patterns of LULC types and their

variations are closely linked with land surface temperature (Wang et al., 2015; Barsi et al., 2014; Weng et al., 2004). These changes can have a detrimental impact on landscape beauty, energy efficiency, human health, and urban quality of life (Yue et al., 2007).

NDVI has been proposed as an indicator in the investigation of the connection between LST and vegetation utilizing remote sensing and ground-based observation in several research (Balew, 2018; Haylemariyam, 2018). Ethiopia calculated the LST's total rise. The NDVI is a straightforward numerical indicator that may be used to assess changes in plant cover and photosynthetic activity. The fact that photosynthetically active vegetation reflects more NIR and less heat energy, respectively, is taken advantage of by combining LST with the NDVI method. Sparsely wooded or deforested regions, on the other hand, reflect less NIR and more heat radiation. However, there has been little research on comparing decadal forest changes in Jimma city and its surroundings, as well as measuring the impact of such changes on land surface temperature. Because the forest cover surrounding the town has been severely impacted by the town's expansion, this location was chosen. On the other side, the population of Jimma city is fast rising, and built-up areas are expanding. LST has been rising as a result of urbanization and inappropriate land use and management, as well as associated issues, resulting in a variety of socioeconomic, environmental, and climatic issues.

1.3. Objectives of the study

General objective

The main purpose of this study was using geospatial tools to assess the impact of changing forest cover on land surface temperature in Jimma and its surroundings from 1987 to 2019.

Specific objectives

- To analyze the relationship between LST and land use and land cover change.
- To examine the temporal and spatial change in LST as a function of LULC changes.
- To examine the effects of LULC changes on the research area's land surface temperature.

1.4. Hypothesis

1. Ho: there is no association between forest cover change and land surface temperature.

   H1: there is an association between forest cover change and land surface temperature.

2. Ho: NDVI and NDBI variables have no significant effect on land surface temperature.

   H1: NDVI and NDBI variables have a significant effect on land surface temperature.

1.5. Significance of the study

As Jimma city is the fast-growing city in the Oromia regional state, forest cover changes have been proportionally rapid. Such fast change in the landscape affects forest cover of the area and causes land surface temperature increase; and therefore, Forest cover change planning and LST mitigation, adaptation strategies, and options. To see the change in LST, the types of LULC and their changes have to primarily analyze through applying change detection analysis. Here, satellite data and remote sensing techniques play a great role. Thus, preparing an up-to-date LULC map helps for proper LULC planning and environmental protection. The result of this study will also be used in decision-making and planning concerning mitigation measures of the impacts of forest cover change. Furthermore, the study is significant to analyze Spatio-temporal variations of LST, how it may change and why it changes; examine the relationship between LST with NDVI and NDBI. Information obtained from this study may also be used for spatial planning especially land management. Therefore, the result of the study can be used by researchers, environmental planners and experts, policymakers, and other stakeholders.

1.6. Scope of the study

Jimma city and its surroundings, which include the Awetu watershed and Jimma city in Jimma zone, Oromia regional state in South West Ethiopia, are the subject of this research. Bore, Kofe, Gudeta Bula, Bebela Kara, Kejomeje, Gubbe Muleta, Doyo Bikila, Doyo Toli, and Semoyu, as well as Jimma city, make up the research area, which covers 24,915.13 ha.

1.7. Organization of the paper

The thesis was organized into five chapters; chapter one presents the background of the study, statement of the problem, objectives of the study, significance of the study, and

scope of the study. Chapter two presents the literature review, where a general review of current knowledge relevant to the research topic is provided. Chapter three describes a description of the study area and the methodology used in the study and data collection techniques. Chapter four explains the results and discussion, which presents the detailed results and discussion. In this section LULC maps generated using maximum likelihood classification, LST, NDVI, and NDBI results were presented. Moreover, change analysis of LULC and LST, correlation, and regression analysis were outlined and discussed. Finally, the conclusions drawn together with recommendations are presented in chapter five.

CHAPTER TWO

2. LITERATURE REVIEW

2.1. Concepts and definition of terminology

Human-induced causes such as deforestation, agricultural activity, and urbanization have significantly altered the earth's surface during the last several decades. Land is the biosphere's ultimate resource, and the term LULC has been used in a variety of studies. These two words, however, refer to two distinct situations and have different meanings. The observable biophysical cover on the earth's surface, comprising water bodies, plant, soil, and hard surfaces, is referred to as land-cover. Land use is the exploitation/utilization of land by humans for settlements, agriculture, forestry, and grazing, which alters land surface processes such as biogeochemistry, hydrology, and biodiversity (Di Gregorio and Jansen, 2000). In this context, variation in the surface component of the landscape and is only considered to occur if the surface has a different appearance when viewed on at least two successive occasions (Lemlem, 2007). The definition also given by FAO (1999) for land-use is as the arrangements, activities, and inputs people undertake in a certain land cover type to produce change or to maintain it. According to Lambin and Meyfroidt (2010), transition in LU/LC can be caused by negative socio-ecological feedback that comes from a rigorous (severe) degradation in ecosystem services as a result of socio-economic changes and innovations.

2.2. Forest, Forest use, and Cover Change

Forests are one of the planet's most valuable hereditary resources. Land having a tree canopy cover of more than 10% and an area of more than 0.5 ha is referred to be forested land (FAO, 2000). World Bank-funded woody biomass investment and strategy planning (WBISPP, 2004) also defines forest as “a relatively continuous cover of trees, which are evergreen or semi-deciduous only being leafless for a short period, and then not simultaneously for all species the trees should be able to reach a minimum height of 5 m.” Forests are determined both by the presence of trees and the absence of other predominant land-uses.

Forests are valuable resources that provide economic, environmental, recreational benefits and provide a wide range of items. Wood from forest trees is used to make furniture and hand tools, as well as lumber and play wood. The primary source of fuel for cooking and heating is wood obtained from the forests (Chala, 2010).

Rao and Pand (2001) observed that forests manage local and global climate, mitigate weather events, regulate the hydrological cycle, preserve watersheds and their vegetation, water flows, and soils, and regulate the hydrological cycle. Forest trees and other green plants produce oxygen as they prepare their food. Almost all life would come to an end if green plants did not continually replenish the oxygen supply. Carbon dioxide rises in the atmosphere, on the other hand, may drastically affect the earth's climate. Forests also provide as a haven for a variety of wild creatures, birds, insects, and plants that would otherwise be unable to survive (David & Corin, 2001).

Despite all these advantages, forest cover lands all over the world in general and in Ethiopia in particular, have been modified and converted into other land use or land cover system. Forest cover change is a way in which the level of diversity and the density of individual species that make up dense vegetation structures are altered as a result of both natural and human factors (Williams, 2003). The causes of forest cover change are complex and dynamic. There is stiff competition in the global economy which drives the need for more money in the economically challenged tropical countries, with most the tropical forests. Deforestation is a result of the interaction of environmental, social, cultural, and political forces in a given region.

According to Elijah (2007), the three main causes of deforestation in the world are; agriculture (including huge investment), infrastructure expansion, and wood extraction. He asserted that the action of human beings rather than natural forces is the source of most contemporary change for this dynamic world.

2.2.1. Land surface temperature

Land surface temperature (LST) denotes the temperature on the surface of the earth or it is the skin temperature of the earth's surface phenomena (Kayet *et al.,* 2016). From the satellite's point of view, the 'surface' looks different for different areas at different times (Kumar & Singh, 2016). Remote Sensing and geospatial tools play a crucial role in

quantifying and estimating LST. The land surface temperature can be derived from geometrically corrected Landsat thermal infrared (TIR) band 6 and Landsat 8 thermal infrared (TIR) band 10 and 11 (Khin *et al.,* 2012). The LST of a given area can be determined based on its brightness temperature and the land surface emissivity, which is calculated by applying the split-window algorithm (Rajeshwari & Mani, 2014). According to Kerr *et al*. (2004), LST gives information about the difference of the surface equilibrium state and vigorous/vital for many applications. LST is also defined as, the monitoring of surface temperature based on pixel-derived observation through RS (Paramasivam, 2016). The characteristics of urban LST are depending upon its surface energy balance, which is governed by its properties such as orientation, sky and wind, openness to the sun and radioactive ability to reflect solar and infrared, and also ability to emit infrared availability of surface moisture to evaporate and roughness of the surface (Voogt, 2000). LULC changes due to changes in surface temperature (ST) which makes both urban and rural managers estimate the urban ST and its surrounding rural area for urban planning as well land management in general (Becker & Li, 1990).

2.2.2. Normalized difference vegetation index

Normalized difference vegetation index (NDVI) is an index based on the spectral reflectance of the ground surface feature. Each feature has its characteristic reflectance varying according to the wavelength. NDVI can be developed using near-infrared and red bands of the remote sensing data and value ranges between -1 to +1. A higher value of NDVI (close to +1) infers the presence of healthy vegetation in the area while its lower value (-1) is the indicator of the absence of vegetation. Hence, the NDVI is very crucial induces for assessing the health of vegetation, the greenness of the earth's surface, crop monitoring and yield forecasting, and forest cover assessment and deforestation and desertification. The normalized difference vegetation index is very essential used for analyzing and mapping land-use and land-cover (Ahl *et al*., 2006; Huang & Siegert, 2006; Woodcock *et al.,* 2002). Furthermore, NDVI is very essential for analyzing the urban green environment and urban climate since it indicates the level of dryness and warmness of the area.

2.2.3. Relationship of land-use types with normalized difference vegetation index and land surface temperature

Land surface temperature, normalized difference vegetation index, and land surface emissivity are significant factors in energy budget assessment, land cover valuation, and other related studies to earth surface characteristics (Fei *et al.,* 2016). This provides a better understanding of the overall LULC classes and environmental studies. NDVI and land surface emissivity can be used to assess and evaluate the spatial relationship between LST and different LULC in urban areas and environments (Maimatiyiming *et al.,* 2014).

Land surface temperature varies in LULC types (Haylemariyam, 2018; Igun & Williams, 2018; Sun *et al.,* 2012), for instance, urban green spaces have high NDVI and low LST than industrial zone. The LST has inversely related to NDVI (Sun *et al.,* 2012; Jianga & Tiana, 2010; Yue *et al.,* 2007). This means that the higher the NDVI value the lower the value of surface temperature and the lower the NDVI the higher the LST. This indicates that the spatial distribution of LST and NDVI varies with the variation of LULC types (Yue, *et al.,* 2007; Weng, *et al.,* 2004; Wilson, *et al.,* 2003). For example, LST increases with the expansion of built-up areas (Sun *et al.,* 2012; Jianga & Tiana, 2010) while the normalized difference vegetation index is lower. Therefore quantifying and assessing the interrelationship of LST and NDVI is very important for evaluating environmental influences in urban ecosystems (Wilson *et al.,* 2003).

2.3. Empirical review

2.3.1. Global forest cover change

Today, the human being has taken the leading role in changing natural environment and there is increasing pressure on these nonrenewable natural resources. So making suitable or harshen it is in our own hands, i.e. our activities have essential in a modification of the physical or man-made environment.

According to FAO (2012) and UNEP (2011), the world population has become above 6.5 billion and is expected to double in the next 50 years. Forests maintain conditions that make life possible. Forests also play an important role in the global carbon balance, as both carbon sources and sinks. They have the potential to form an important component to combat global climate change. When forests are transformed into agriculture, the

subsequent land-use systems are implemented to determine the amount of carbon sink potential that takes place. But, now it was threatened with elimination.

The land cover transformation did not stop, but rather accelerated and diversified with the onset of Urbanization, the industrial revolution, the globalization of the world economy, and the expansion of population and technological capacity. Plant and animal species become thinned; grasslands plowed or grazed; croplands and cities expanded; wetlands drained and forests cleared for millennia, yet never so rapidly worldwide as at present. (Mather, 2014)

Although the magnitude of deforestation in the tropics, particularly in developing countries varies substantially, available data suggest that deforestation is a real trend. Large forests have been transformed for farm and settlement developments. This shows that people have assumed that rich vegetation is a sign of the fertile soils that lie under the forest, and this has lead to rapid forest clearance for agriculture as well as timber supply.

In the tropical region, many types of forest cover are now rapidly declining because of mismanagement and the slash and burn practices of the increased human population. In the meantime, literature indicated that as many as 20 million ha of tropical rainforest are destroyed each year and most of this destruction has occurred in Africa, Asia-Oceania, Central America, and South America. Concerning this, Asner *et al.,* (2009) have stated that in the year between 2000 and 2005 gross deforestation was 0.5%, 1.3%, 1.4%, and 1.8% in Africa, Asia-Oceania, Central America, and South America, respectively. This sums to a loss of about 274,615 km^2, or 1.4%, of global humid tropical forests in just 5 years. Matthews (1982) estimated that the pre-agricultural closed forest once covered 46.28x106 km^2 of the globe, and woodland some 15.23x106 km^2 being reduced to 39.27x106 km^2 and 13.10x106 km^2 respectively by the end of 20^{th} century.

Start from the past millennium and still today humans have taken an immense role in the modification of the global environment. With increasing numbers and developing technologies, man has emerged as the major actor, the most powerful and universal instrument of environmental change in the biosphere today.

2.3.2. Extents of forest cover in Ethiopia

Ethiopia owns diverse vegetation resources, from tropical rain and cloud forests in the southwest and on the mountains to the desert scrubs in the east and northeast and parkland agroforestry on the central plateau (Demel, 2010).

The vast terrestrial land surface with biologically productive climate and soil indicates the country has a huge forestry development potential. The forest resources are an important endowment of the country. They contribute to production, protection, and conservation functions.

Ethiopia‟s flora and fauna resources are uniquely diverse. The flora comprises about 6500-7000 species of higher plants out of which 12% are endemic and the countries natural forests and woodlands covered 15.1 million ha in 1990 (EARO, 2008).

In 2005, the forest cover had further declined and was estimated to cover 13.0 million ha. In other words, Ethiopia lost over 2 million ha of forests, with an annual average loss of 140 000 ha between 1990 and 2005. In 2009, the area is estimated at 12.3 million ha, 11.9 % of the total land area. Of this, the remaining closed natural high forests are 4.12 million ha or 3.37% of Ethiopia‟s land (FAO, 2010).

However in February 2015, Ethiopia adopted a new forest definition as follows: 'Land spanning at least 0.5 ha covered by trees and bamboo), attaining a height of at least 2m and a canopy cover of at least 20% or trees with the potential to reach these thresholds in situ in due course‟ (MEFCC, 2015).

This forest definition differs from the definition used for international reporting to the Global Forest Resources Assessment (FAO) and from the forest definition used in the National Forest Inventory which both applied the FAO forest definition with the thresholds of 10% canopy cover, a 0.5 ha area, and a 5 m height.

The reason for Ethiopia to change its national forest definition is to better capture dry and lowland-moist vegetation resources. In specific, the reason for lowering the tree height from 5 to 2 m is to capture Termilania-Combretum dense woodlands found in Gambella and Benishangul Gumuz Regional States which in its primary state consists of trees reaching a height of around 2-3 m and above. The proposed change in forest definition

results in the inclusion of what previously was classified as Ethiopia‟s dense woodlands which have a wider distribution through the country (MEFCC, 2016). After this definition, the forest cover of Ethiopia is 12.5% (FAO, 2015).

2.3.3. The causes of forest cover change in Ethiopia

In Ethiopia, forest cover change is often more complex than simply deforestation. Wogderes (2014) and Ariti, *et al*., (2015) confirmed that the high demand for agricultural land due to the growing human population has contributed to the deterioration and depletion of forest resources of the country. Most recent studies reported the decline of natural vegetation including forests, shrubs, and woodlands due to conversion to agricultural and grazing lands, the demand for fuelwood and construction materials, repeated fire outbreaks, and opening up settlements areas in different parts of the country (Alemu *et al.,* 2015; Ariti *et al.,* 2015).

Now a day's much more damages have been done to the forest resources of Ethiopia. With their axes, a group of people can destroy dense forests to get fresh farms and grazing lands. The use of forests as traditional sources of energy is one of the major causes of deforestation in Ethiopia. Fuelwood accounts for the bulk of the wood used in the country and it is the fundamental domestic energy source for people who are living in both urban and rural parts of Ethiopia (Zeleke & Hurni, 2001).

Besides, the shifting of the political center from place to place in the past was an important determinant factor for the problem of deforestation in Ethiopia. Historical source's indicated that the movement of the political center from Axum in the North via Gondar to Addis Ababa was related to the royal camp's need for wood for fuel and building material. Concerning this (Harvith, 1968) findings indicated that before Addis Ababa become a permanent capital of Ethiopia there were other many capital towns. As a result, the kings and rulers with their followers move from place to place to hear complaints from the people and to check some rebellions tribes. Thus, the location of their capitals changes three to four times during a year. These frequent changes of residence were not only due to the above-mentioned political and social reasons but also resource exhaustion, mainly forest resources.

On top of this, the introduction of the sawmill industry and their uncontrolled activity is to a large extent responsible for the massive destruction of forest resources, and large areas were selectively exploited without reforestations (FWCDA, 1982).

To sum up, rapid population growth along with the need for farming and grazing land, movement of political capital in the country for a long period, the need for fuelwood and building materials, forest fire, and the introduction of sawmill industry are the major contributing factors for the transformation of forest cover land into other land use and land cover systems in the country.

2.3.4. Impacts of forest cover change on land surface temperature distribution

Population expansion and its spatial distribution have an impact on the destruction of Forest cover and exhaustive use of land (Jianga & Tiana, 2010). This affects the ecosystem of the earth's surface and reduction in plant species biodiversity. Forest cover change, therefore, has a great impact on the change and distribution of land surface temperature. For instance, because of low evaporative cooling and low heat transfer capacity of bare land especially salinized soil domination has a high surface temperature. Besides, the modification and change of vegetation cover, agricultural and grazing land, and water bodies have a great influence on the changes and variation of the earth's surface temperature (Fei *et al.,* 2016).

Though forests have an extensive influence on local, regional, and global climates, loss of forest due to deforestation results in increased insolation; decreased cloudiness and approximately compensating the effect of cloud; amplified reflectance of the land surface; change the large-scale convergence of atmospheric moisture which influence precipitation and modify rainfall patterns; and changes in surface roughness and wind speeds and direction (Yadvinder *et al.,* 2008). Deforestation also contributes directly and indirectly to the loss of terrestrial marine ecosystems. Therefore, it accelerates diminution of forest area, loss of complexity and diversity (Donato *et al.,* 2016) as well as affect volume of water, increase surface water heat due to sedimentation, and rise evaporation. Besides, it increases in soil and land degradation, desertification (Abbas *et al.,* 2010; Temesgen *et al.,* 2014), wetland degradation and cause for fluctuation of rainfall and humidity, and change surface

temperature. This instability affects the thermodynamic processes at the earth-atmosphere interface and the dynamic processes in the atmosphere.

Deforestation also increases greenhouse gases (GHG) emission, for instance, carbon-di-oxide, methane nitrous oxide, and others into the atmosphere (Rajeshwari & Mani, 2014), increases albedo and decreases canopy roughness (Peter, 1994), minimize rainfall availability, and increase surface temperatures (William & Turner, 1992). This increases the land surface temperature of the surface of the earth. Consequently, the change in the value of land surface temperature changes the climate and its elements.

Rapid urban expansion and industrialization increase buildings, gases released from vehicles and industries (Manea *et al.,* 2013), non-evaporating impervious surfaces like concrete and asphalt (Jianga & Tiana, 2010; Qijiao & Zhixiang, 2015; Tang *et al.,* 2014), which heats the urban environment directly. Subsequently, urbanization leads to the reduction of green spaces in urban areas (Jianga & Tiana, 2010), which modifies urban surface water content and vegetation cover (Qijiao & Zhixiang, 2015; Tang *et al.,* 2014). The physical change of the urban surface (albedo, thermal capacity, heat conductivity) can affect urban surface temperatures by altering the sensible and latent heat exchange between the urban surface and boundary layers (Mohan & Kandya, 2015). Therefore, these urban biophysical changes increase UHI (Fenglei *et al.,* 2009; William & Turner, 1992) a phenomenon of higher atmospheric and surface temperatures occurring in urban areas (Gluch *et al.,* 2006). These are responsible for climate change (Zheng *et al.,* 2014) and increasing energy consumption. Finally, these bring global warming at local, regional, and global scales.

2.4. The role of remote sensing and GIS for forest cover and land surface temperature analysis

Remote sensing and GIS techniques have been widely used over the world for the study of historical changes in Forest cover change and LST analysis. Remote sensing has been used to identify vegetation cover, air pollution, LST, and other surface characteristics (Weng *et al.,* 2004). In this regard, remote sensing has been playing a crucial role in provides satellite imageries to assess natural resources and monitor environmental changes. For example,

Landsat is one of the satellites which providing synoptic, repetitive, and global coverage data freely since 1972. Landsat imageries have been used for various terrestrial applications. Therefore, Remote Sensing allows analyzing land-use and land-cover change dynamics using time series of remotely sensed data by integrating it with socio-economic or biophysical data. Remote sensing is also efficient in land-cover mapping, detecting and monitoring land-cover change over time and space, identifying land use attributes, and land cover changes hot spots (Abate, 2011; Abbas *et al.,* 2010; Temesgen *et al.,* 2014). With the advancement of technology, reduction in data cost, availability of historic Spatio-temporal data, and high-resolution satellite images, remote sensing technologies are now very useful for conducting land cover change detection analysis and predicting the future scenario (Agarwal *et al.,* 2002).

Moreover, land surface temperature and NDVI can be easily computed by using satellite data specifically thermal remote sensing is very crucial for assessing and measuring urban thermal environment (Sun *et al.,* 2012; Yue *et al.,* 2007). It also provides a tool for analyzing thermal variation measurements of physical, environmental, and socioeconomic variables in urban settings (Small, 2004). Remote sensing data is also significant for analyzing the relationship of LULC change with LST and NDVI. Therefore remote sensing is very useful for studying the urban environment (Yue *et al.,* 2007) and the rural environment as a result, it is possible to extract information about the earth's surface from the satellite imageries and analyze and make an informed decision.

Previously, different researchers outside Ethiopia did researches on the impact of LULCCs on LST. However, in Ethiopia, there are some papers related to the proposed title. For example, (Gebrekidan, 2016) studied modeling land surface temperature from satellite data, the case of Addis Ababa. The study mainly focuses on modeling the LST of Addis Ababa city, which acquired Landsat 5 and 8, from 1985 and 2015. Finally, the results show that a negative correlation was found between NDVI and LST and the study indicates the need for urban greening and plans to increase vegetation cover to sustain the ecosystem of the city and to minimize the urban heat island effect. The study carried out by (Haylemariyam, 2018) in Dire Dawa city focuses on the Detection of Land Surface Temperature concerning Land Use Land Cover Change by acquiring TM, 1993, and

OLI/TIRS, 2017 Landsat images. It showd that LST and NDVI are negatively correlated. According to Streutker (2003), one of the promisings of studying urban surface temperature is using remote sensing or air-born technology. Evaluation of land surface temperature from remotely sensed data is common and typically used in studies of evapotranspiration and desertification processes. The wide use of land surface temperature for environmental studies has made remote sensing of land surface temperature an important academic issue during the last decades. Indeed, one of the most important parameters in all surface-atmosphere interactions and fluxes between the land and the atmosphere island surface temperature.

2.5. Literature gap

To support forest resource conservation and decision-making, new tools, methodologies, and practices for monitoring above-ground biomass are now required. To control land surface temperature, new technology and mapping systems should be used to guide above-ground biomass conservation, development, and management. However, because information on vegetation resources is fragmented throughout Ethiopia, it is difficult to obtain reliable information on their coverage, distribution, change over time, growing stock in standing vegetation, and regeneration.

Besides the study carried out in Ethiopia related to Land Surface Temperature detection tries to apply the NDVI method and analysis the result but neglecting the integration of NDBI with multi-spectral satellite imagery (Abebe, 2018; Balew, 2018; Haylemariyam, 2018 & Asfaw, 2017).

Therefore, this study tries to integrate both NDVI and NDBI with meteorological data to see the effect of LULC change on land surface temperature over decades.

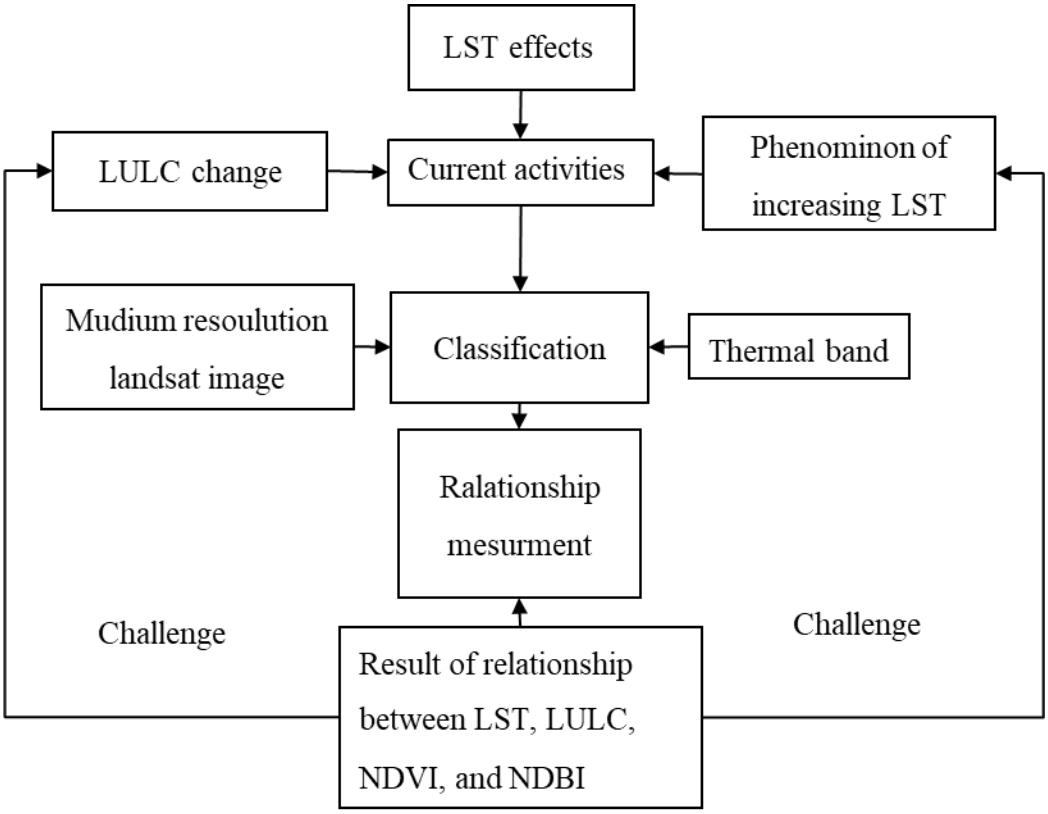

Figure 1: Conceptual framework of the study

CHAPTER THREE

3. MATERIALS AND METHODS

3.1. Description of the study area

3.1.1. Location

The study area includes Jimma city and its surroundings which is one of the oldest and historic cities in Ethiopia. It is found in in Jimma zone of Oromia National regional state, (Figure 2) and located 346 km to the Southwest of the Ethiopian capital, Addis Ababa. The geographical location of the study area extends from 7º 38' 0"N to 7º 46' 0"N latitude and 36º 42' 0"E to 36º 54' 0"E longitude. The study area has a total area of 24,915.13 ha, from which the terrestrial part was about 14,281.13 ha and 10,634 ha is the area of Jimma city.

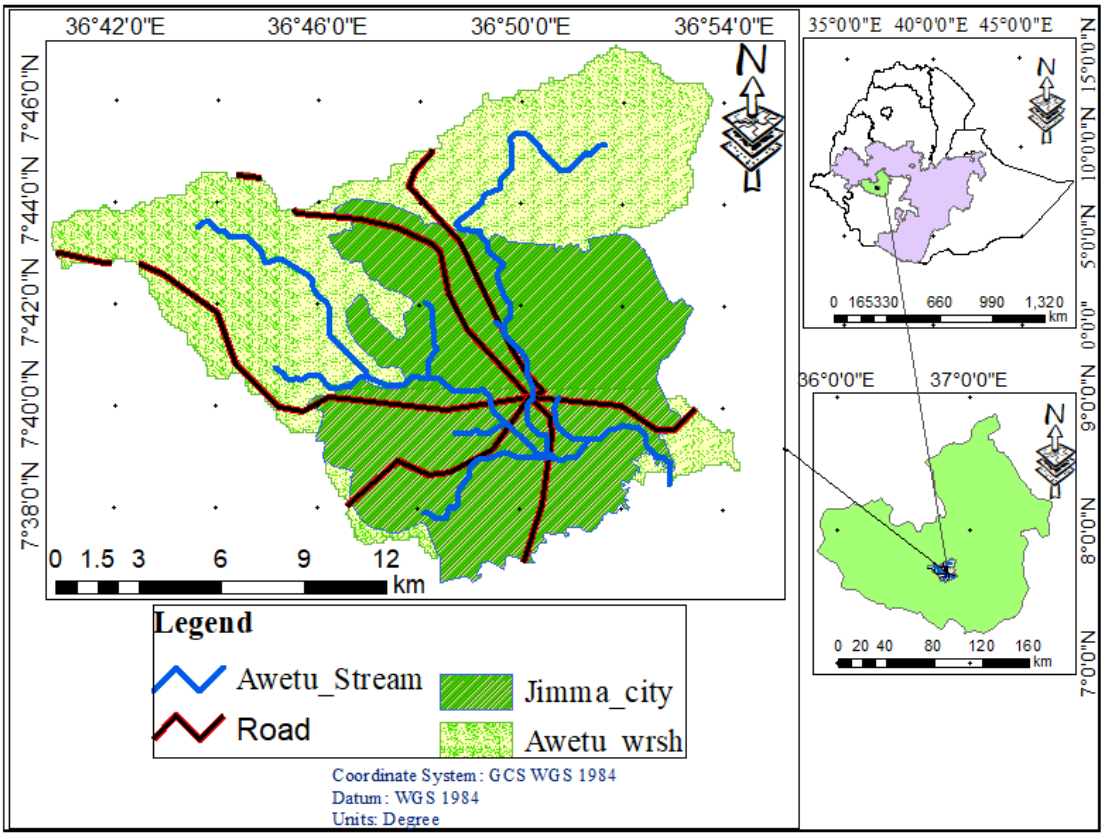

Figure 2: Locational Map of the Study area

3.1.2. Demographic features

According to CSA(1994), the total Population of Jimma City and nine rural villages within the awetu watershed was 88,867, out of these 43,874 (49.4%) were male and 44,993 (50.6%) were female. However, according to the 2007 Population and Housing Census of Ethiopia, the total population of the study area in the year 2007 was 120,960, out of which male 60,824 (50.24%) and female 60,136 (49.76%). This indicates that the population of the study area has been growing at the rate of 2.3% per annum during the period between the two censuses. According to CSA (2013), the total population of the study area was 195,228 out of whom 97,259 (49.8%) were male and 97,969 (50.2%) female (Figure 3).

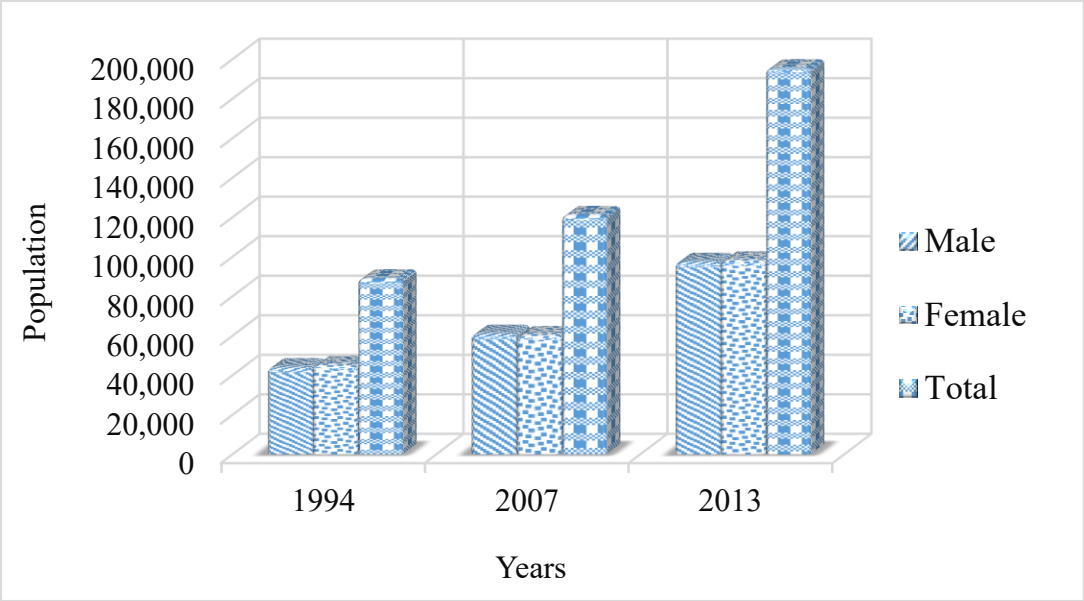

Figure 3: Population distribution of Jimma city and its surrounding (1987-2019)

3.1.3. Socio-economic features

According to the report of the Finance and Economic Development Office of Jimma city (2010), the main economic activities in the city were commerce and small-scale manufacturing enterprises. The local urban-rural exchange in the area has contributed to significant business activities in Jimma. The industries in the town are small-scale and cottage industries like grain mils, wood and metal workshops, coffee hullers, hollow block manufacturing, bakeries, and pastries. The dominant manufacturing activities that account

for 70% of the total number of manufacturing enterprises in the city are grain mills and woodworks.

3.1.4. Topography

Jimma city and it's surrounding lies between the lower point, 1676 meters above sea level in the southern part, and a higher point to 2581 meters above sea level in the western and eastern part.

Slope can be defined as the upward or downward inclination of a natural or artificial surface or it is a deviation of the surface from the horizontal. According to FAO (2006) classification, the slope of the study area has been categorized into five classes as indicated in (Figure 4).

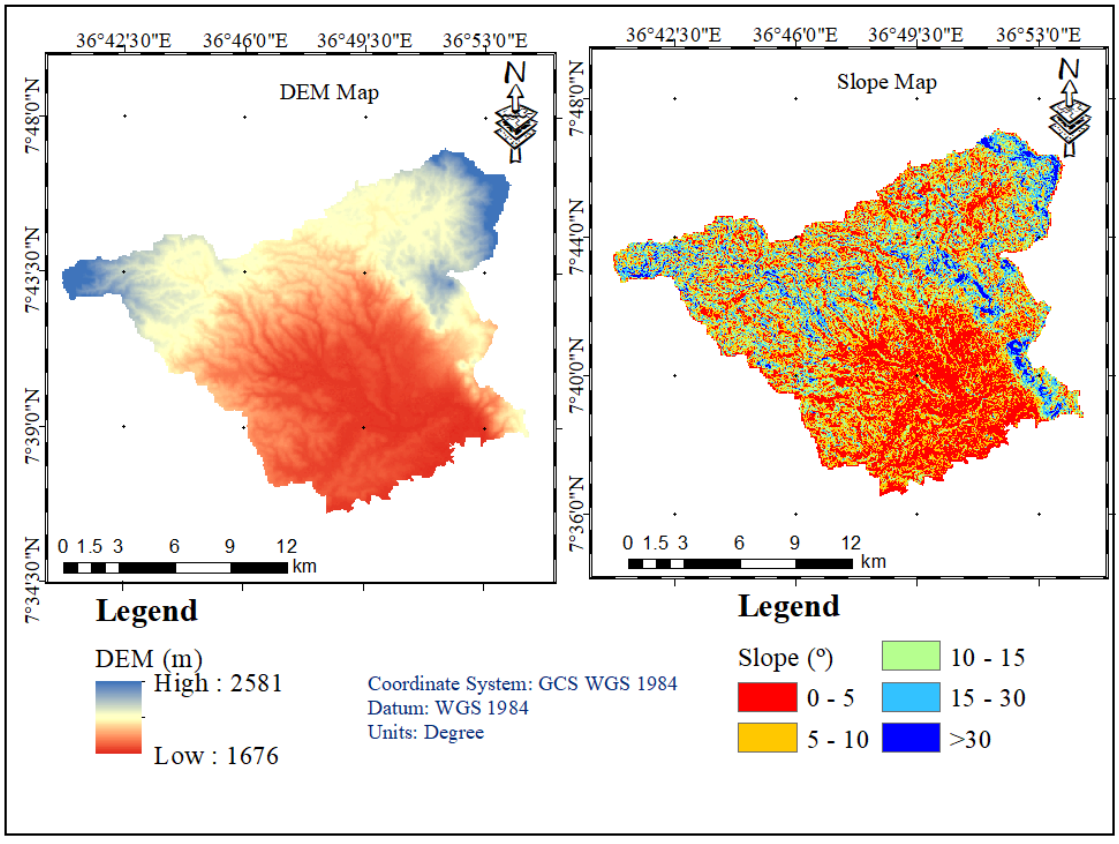

Figure 4: Elevation and slope map of the study area.

Source: ASF

3.1.5. Climate

The study area is characterized by a tropical humid climate that has high precipitation, warm temperature, and a long wet period (Western Oromia region Meteorology Center, 2019). According to thirty-two years of rainfall data collected from the western Oromia region meteorology center (WORMC), the mean annual rainfall of the Jimma city and its surrounding from 1987-2019 ranges from 913.3 mm to 2935.58 mm. As indicated in Figure 5, during 32 years of the study periods, the mean annual rainfall was varying from year to year, mostly due to the variations of climate and weather parameters. Although the Jimma city and its surroundings have almost all year-round precipitation, the maximum recorded annual rainfall was in 1996 and the minimum annual rainfall record was in 2018. Agro climatically, the area is largely woina dega type covering about 47% of the total area, 35%, and 18% are in dega and kola zones respectively (WORMC, 2019).

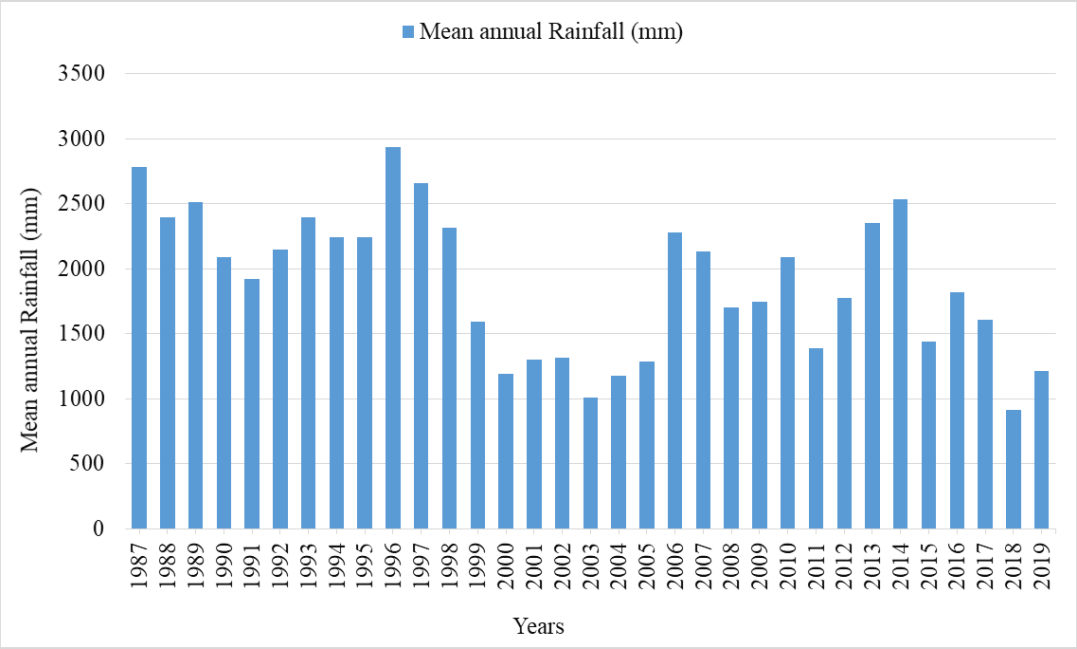

Figure 5: Mean annual rainfall of the study area.

Source: (WORMC, 2019)

The mean annual temperature of the study area is between 12ºC and 29ºC with a mean daily temperature of 19.5ºC. The maximum mean annual temperature of 26.26ºC in the

study area was recorded in 2003 and the minimum mean annual temperature of 13.7ºC was recorded in 2007 (WORMC, 2019).

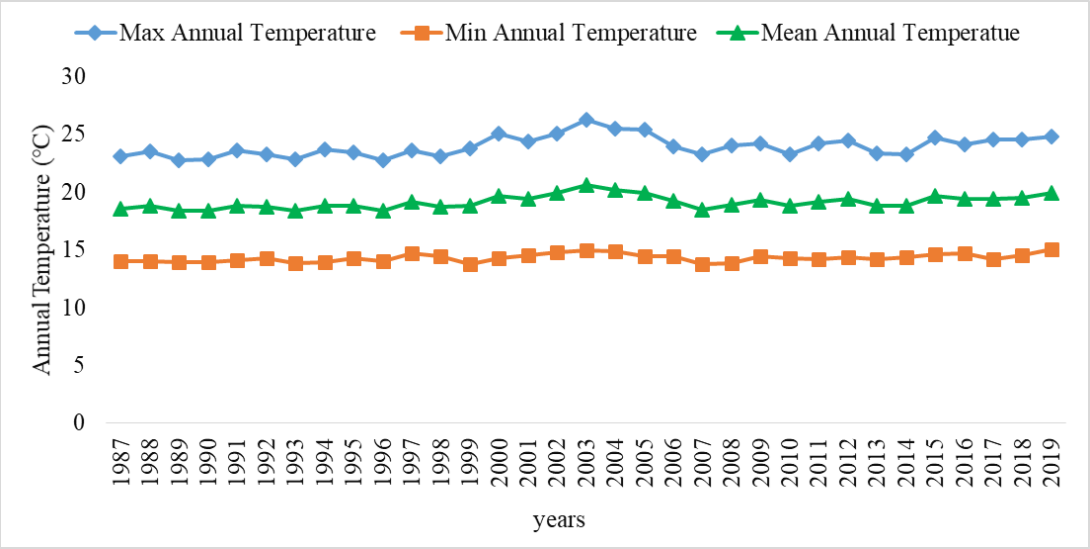

Figure 6: The annual temperature of the study area

Source: (WORMC, 2019)

3.1.6. Soil

According to FAO (2006) classification, the Jimma city and its surroundings have six major soil classes. They are dystric nitisols (56.9%), eutricfluvisols (26.8%), dystric fluvisols (10.3%), chromic vertisols (3.6%), orthicacrisols (1.3%) and eutricnitisols (1.1%). Generally, the soils are reddish-brown and shallow at higher altitudes, while at lower sites they tend to become gray and deep (Figure 7).

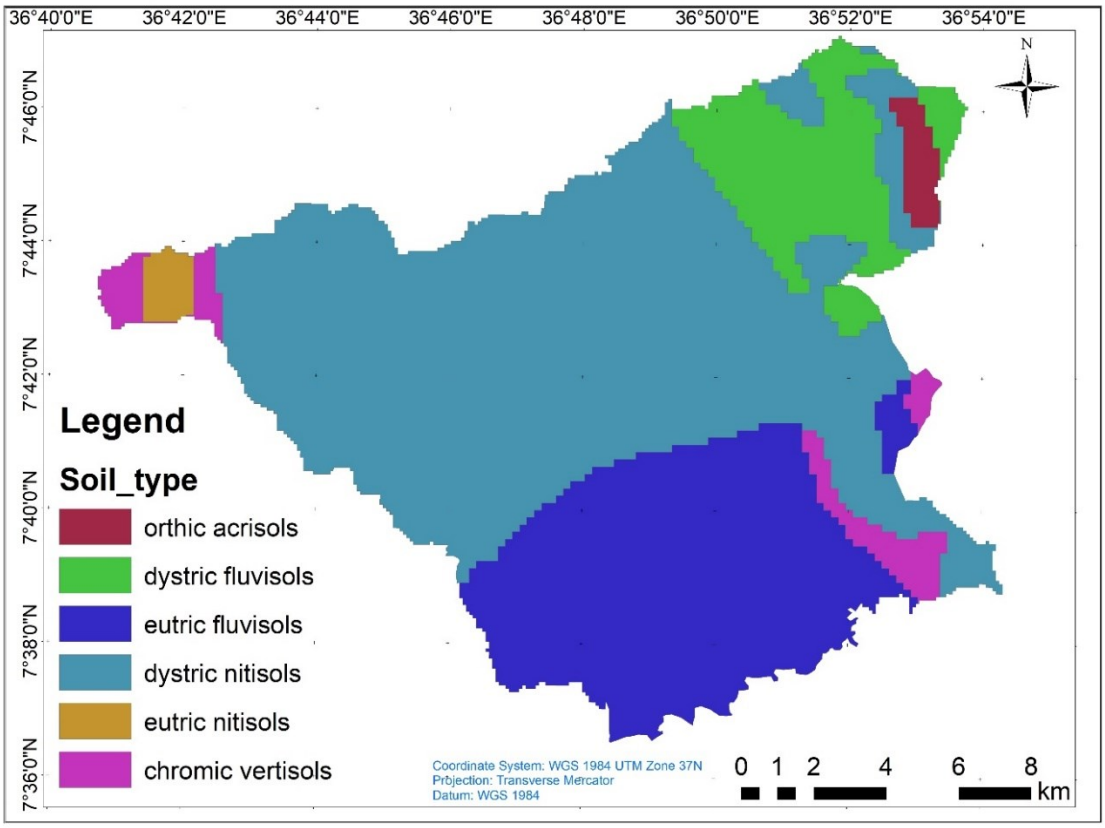

Figure 7: Soil Map of the study area

3.2. Design of the study

The causal research design was employed for the study because it attempted to reveal a cause-and-effect relationship between two variables. The LULC of the study area change matrixes was done quantitatively and after that, the LST of the study area derived from the Landsat image was also done quantitatively finally the two results were taken for relationship analysis.

The procedure that was followed in this study is presented using the flow chart (Figure 9). It shows the steps followed beginning from the acquisition and classification of a multi-temporal satellite image of the study area to extract the required information. The first step was LULC analysis from Landsat 5, 7, and 8. Second estimation of LST from Landsat imageries. Finally, correlation statistics were done for NDVI, NDBI, and LST. Relationship analysis was done for LULC and NDVI, and LULC and LST.

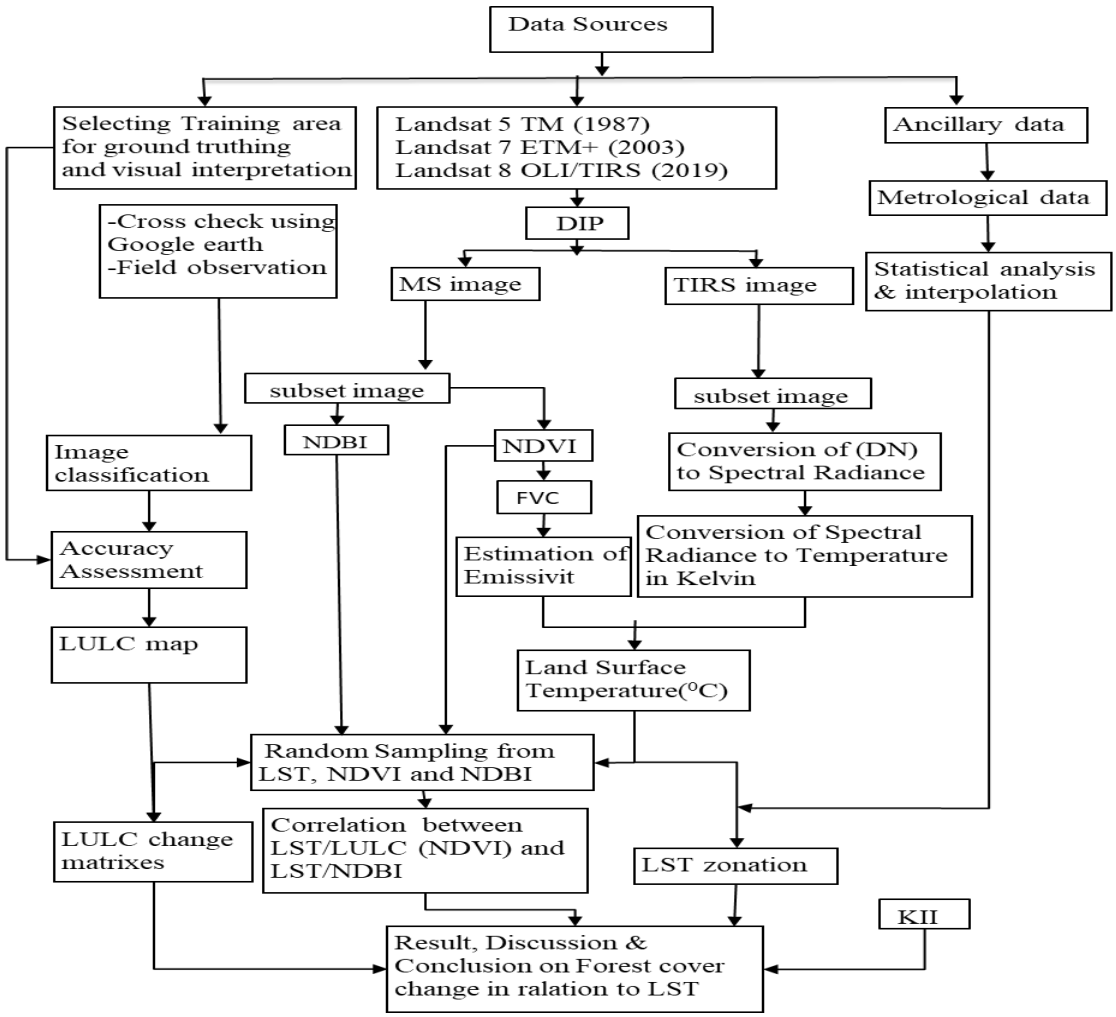

Figure 8: Methodological flow chart.

3.3. Data type and source

To reach the desired goal the study was used both primary and secondary data types.

I. Primary data: The research was conducted using unstructured key informant interviews and a field survey. Unstructured key informant interviews were conducted with nine elders from each sampled village with the goal of determining the primary cause of forest cover change and its impact on urban temperature. Field surveys were conducted using Global Positioning System (GPS Garmin 72) to generate primary information regarding identifying the existing land-use type of the study area. Google Earth map was used as a base map for image classification. It was also used to extract reference points for inaccessible areas and for the image of 1987 and 2003.

II. Secondary data: the study was used different secondary data to identify the land-use type, NDVI, NDBI, and analyzing the land surface temperature of Jimma city and its surrounding. Geospatial data and literature survey data that were obtained from different sources were used for this study. Digital geospatial datasets in raster formats that were collected from various sources for the preparation of factor maps this includes:-

- Landsat images of 1987, 2003, and 2019 of the study area were used to analyzing of LULC change, NDVI, NDBI, and LST distribution of the study.
- Meteorological data such as temperature and rainfall data were used to describe the climate of the study area during the study periods

Many literature reviews data were collected using the internet, others were collected from books and reports, and all literature was categorized according to the research topic.

3.3.1. Meteorology Data

The Western Oromia region Meteorology Center provided meteorological data like as temperature and rainfall. The climate of the study area throughout the study periods was described using temperature and rainfall data.

3.4. Materials and tools

Image digitization, split and merge polygons, zonal statistics, reclassification, LST mapping, and mapping NDVI and NDBI were all done with Arc GIS 10.4.1 software. Multi-temporal satellite images were processed using ERDAS IMAGINE 2015 software, which included image correction, enhancement, and processing (classification for LULC mapping and change calculation, LST calculation, and NDVI and NDBI generation). The correlation statistics of LST, NDVI, and NDBI were developed using SPSS software.

3.5. Methods of data collection

3.5.1. Remote sensing data

The three sets of remotely sensed data used for this study include: Landsat thematic mapper (TM), Enhanced thematic mapper (ETM+) and Landsat operational land imager (OLI), and Thermal infrared sensor (TIRS) images (with path/row 169/55) acquired during the month January 1987, February 2003, and January 2019 were used, because, these months were

relatively free from cloud and haze. Due to the problem of poor resolution of MSS sensor and data availability, the study period covered only from the year 1987 to 2019. Thus, the years 1987, 2003, and 2019 were selected for analysis with 16 years intervals. Detailed descriptions of Landsat datasets that were used for Landsat image sharpening, analyzing of LULC change, NDVI, NDBI, and LST distribution of Jimma city and its surroundings are given in Table 1.

Table 1: Description of data and their sources

Satellite	Sensors	Path & row	Resolution (m)	Acquisitions date	Source of data
Landsat	TM	169-055	30	01/31/1987	USGS
	ETM^{+}	169-055	30	02/20/2003	"
	OLI	169-055	30	01/23/2019	"
Thermal Infrared (band 10)	TIRS	169-055	100	01/23/2019	"
Thermal Infrared (band 11)	TIRS	169-055	100	01/23/2019	"
DEM			12.5 (m)	2019	ASF

3.5.2. Ground Truth Data

A stratified random sample approach was used to conduct a ground truthing activity in the study area, where distinct LULC classes were validated. Agriculture, forest cover, settlement, shrubland, wetland, and water body were rated from largest to smallest in the observed LULC. These LULC classes were utilized to create the map legends, and the training data set for image classification was gathered with the use of GPS. Furthermore, ground truth data was used to measure accuracy. Photos of areas of interest and coordinates from sampled LULC classes were taken during these ground-truthing activities.

.

3.6. Methods of data analysis

3.6.1. Digital image preprocessing

Landsat images for 1987, 2003, and 2019 were obtained from the USGS database using the Thematic Mapper (TM), Enhanced Thematic Mapper (ETM+), and operational land imager (OLI) and thermal infrared sensor (TIRS). Each image was adjusted geometrically and radiometrically as used in (Orimoloye, et al., 2018). The spectral bands were layer stacked to produce a composite image of the study area for each year (1987, 2003, and 2019) for the purpose of LULC classification image analysis. Thermal band 6 for Landsat 5 TM, ETM+ and band 10 & 11 for Landsat 8 TIRS were employed to calculate the LST from all the periods under consideration. The thermal bands have their original pixel sizes of 120 m for TM and 100 m for TIRS images which were resampled to 30 m using the nearest-neighbor algorithm to match the pixel size of other spectral bands. In order to examine the effects of human activities in the study area, a land cover classification was necessary for the detection of LULC changes as a result of rapid urbanization from 1987 to 2019. After selecting training areas, a supervised classification with the maximum-likelihood algorithm was carried out to classify the Landsat images using bands 2 (green), 3 (red), and 4 (near-infrared). Visual image interpretation was done with field knowledge and making reference to Google Earth images of the study area. The error matrixes of the three LULC maps were generated to assess the accuracy of the classification result. To make the data compatible with each other, the projection transformation was carried out and assigned to the WGS_1984 UTM Zone 37 N projection.

Image sharpening: A resolution merging or image sharpening approach was employed to improve the resolution of the images and improve image interpretation. To increase the quality of low spatial resolution multispectral images, utilize high spatial resolution panchromatic images, for instance. The improved Landsat images were visible and better than the original images, owing to a multiplicative_ nearest neighbor method, which was employed among several image sharpening approaches.

3.6.2. Image classification

Image classification is the task of extracting information classes from a multiband (Multi-spectral) raster image or extracting information based on the reflectance of the object and it serves specific aims; which is converting image data into thematic data (Gao, 2009; Richards & Jia, 2006). The information class can be grouped into a thematic layer of having similar LULC in the image. Though there are automated image classification techniques, manual or visual image interpretation procedure was used. This is because there is a problem of pixel mixing especially in low-resolution imageries such as Landsat and this has seriously affected the LULC classification accuracy of the study.

A supervised classification method was used in ERDAS imagine to obtain LULC of the study area. Among different classification algorithms, the maximum likelihood was used for supervised classification by taking the ground control points for six major LULC class categories.

3.6.3. Accuracy assessment

Accuracy assessment is a comparison of image interpretation by a computer with the aid of ground truth data (Gao, 2009; Richards & Jia, 2006). The stratified random sampling approach was utilized to choose the training sites used for accuracy evaluation for this comparison. The groups in stratified sampling are classified based on the similarity of spectral features. To ensure that tiny but essential land covers are included in the sample, stratified random sampling is required (Russell, et al., 2019). A stratum was created for each LULC category. A sample of LULC classification was taken by grouping together many training pixels in the feature space to form a cluster. The clusters should constitute a representative data set for a specific class, as determined by the operator. The number of sample plots (clusters, one cluster's sample size) was 30 n, where n is the number of bands (Wim, *et al.,* 2004). The number of samples was calculated based on the area percentage, although some adjustments were made during the fieldwork to account for physical obstacles and other factors. The sample unit had a 20-meter radius and was part of a cluster of six sample units, including the center, that were 200 meters apart. A total of 210

points were randomly collected from the study area for the 1987, 2003, and 2019 LULC classifications, which is 30 times the number of bands (7).

Overall accuracy was used to calculate a measure of accuracy for the entire image across all classes present in the classified image (Eq. 1). The collective accuracy of a map for all the classes can be described using overall accuracy, which calculates the proportion of pixels correctly classified.

$$Overall\ Accuracy = \frac{\text{Sum of the diagonal elements}}{\text{Total number of accuracy sites pixels (column total)}} \quad \text{Eq.1}$$

Congalton (1991) presented the Kappa coefficient (K) as an additional assessment that may be used in this study in addition to overall accuracy. The K technique is computed by increasing the total number of pixels in all the ground verification classes (N) with the sum of the confusion matrix diagonals (X_{ii}) and subtracting the sum of the ground verification pixels during the class time. The sum of the classified pixels in that class is summed up over all classes ($\Sigma X_i \Sigma\ X_I$), where ΣX_i is the row total and ΣX_I is the column total, and divided by the total number of pixels squared minus the sum of the ground verification pixels in that class times the sum of the classified pixels in that class summed over the classes.

$$k = \frac{\mathrm{N}\sum_{i=1}^{k} x_{ii} - \sum_{i-1}^{k}(x_i * x_I)}{N^2 - \sum_{i-1}^{k}(x_i * x_I)} \quad \text{Eq.2}$$

$$k = \frac{(Total\ Sum\ of\ correct) - Sum\ of\ the\ all\ (row\ total\ column\ total)}{\text{Total squared} - \text{Sum of the all (row total column total)}} \quad \text{Eq.3}$$

In general, the Kappa Coefficient is generated from a statistical test to evaluate the accuracy of classification. Kappa essentially evaluates how well the classification performed as compared to just randomly assigning values, i.e. did the classification do better than random. The Kappa Coefficient can range from -1 to 1. A value of 0 indicated that the classification is no better than a random classification. A negative number indicates the classification is significantly worse than random. A value close to 1 indicates that the classification is significantly better than random.

3.6.4. Land use land cover thematic layer

After classification accuracy was conducted, final LULC were identified and mapped for the three study periods (that is, 1987, 2003, and 2019). So, Jimma city and its surroundings have the following LULC classes.

Table 2: LULC classes and description of the study area

No.	LULC Classes	Description
1	Agricultural land	Areas of land plowed/prepared for growing rain-fed crops. It also includes land with scattered or patches of trees and it is used for grazing and browsing of domestic animals and Areas of land prepared for growing crops.
2	Forest Cover	It represents both natural and fragmented plantation forest areas that are stocked with trees capable of producing timber or other wood products
3	Settlement	The area occupied by house buildings includes road network residential, commercial and industrial, transportation, roads, and mixed urban and other facilities.
4	Shrubland	land supporting an assemblage of small trees and shrubs
5	Wetland	A land area that is saturated with water
6	Waterbody	Areas covered by natural and manmade small dams, like pond and river

Steps or processes that were followed to classify LULC from a Landsat image were presented in Figure 8 below

3.6.5. Change detection

To observe the rate of increase or decrease in the LST over smaller areas, a change detection analysis was carried out. To show the relationship between the LST and the different land cover types, a statistical approach was used to carry out a correlation and regression analysis. This was done using the percentage proportion of the land cover types and their mean LST for 1987, 2003, and 2019, respectively. The percentage proportions of land cover types were classified into vegetated and non-vegetated areas. This is because classifying the land cover types into vegetated and non-vegetated areas helps in estimating the relationship that exists between the LST and the various land cover types. To analyze the total area of LULC changed from 1987 to the 2019 year, the initial and final LULC area coverage was computed following Garai & Narayana (2018) as indicated in Eq.4

$$Rate\ of\ LULC\ change = \frac{(Present\ LULC\ area - Previous\ LULC\ area)}{Previous\ LULC\ area} x100 \qquad \text{Eq.4}$$

3.6.6. Multispectral radiometric correction

Radiometric correction requires converting a remote sensing digital number to spectral radiance values and data for comparisons. Image processing procedures that are used to correct errors, converting a digital number (DN) values to spectral radiance and then reflectance was categorized as a radiometric correction (Prata & Caselles, 1995). To perform the conversion of digital number to spectral radiance equation (5) was used in ERDAS IMAGINE using the formula given by USGS (2019).

$$L_\lambda = M_\lambda * Q_{cal} + A_L \qquad \text{Eq.5}$$

Where; L_λ = Spectral radiance (W/ (m^2 * sr * μm)); M_λ= Radiance multiplicative scaling factor for the band (RADIANCE_MULT_BAND_N from the metadata); AL = Radiance additive scaling factor for the band (RADIANCE_ADD_BAND_N from the metadata); Q_{cal} = Level 1 pixel value in DN.

3.6.7. Thermal atmospheric correction

In radiometric calibration, pixel values, which were represented by Q in remote sensing raw data and unprocessed image data, were changed into absolute radiance values. Hence,

the spectral radiance of TM, ETM+, and OLI images was converted into radiance using the equation (NASA, 2000).

$$L\lambda = \left(\frac{LMAX\lambda - LMIN\lambda}{QCALMAX - QCALMIN}\right)(QCAL - QCALMIN) + LMIN\lambda \quad \text{Eq.6}$$

Where: L_λ = Spectral radiance received by the sensor (W/ (m^2 * sr * μm))

QCAL = the quantized calibrated pixel value in DN

$LMIN_\lambda$ = the spectral radiance that is scaled to QCALMIN (W/ (m^2 * sr * μm))

$LMAX_\lambda$ = the spectral radiance that is scaled to QCALMAX (W/ (m^2 * sr * μm))

QCALMIN = the minimum quantized calibrated pixel value (corresponding to $LMIN_\lambda$ in DN which is 1

QCALMAX = the maximum quantized calibrated pixel value (corresponding to $LMAX_\lambda$ in DN which is 255

3.6.8. Conversion of radiance into brightness temperature

After spectral radiance was converted to radiance, the raw digital numbers of the thermal bands are converted to at-satellite brightness temperatures, which were the effective temperature viewed by the satellite under an assumption of uniform emissivity (Rajeshwari & Mani, 2014).

$$BT = \frac{K2}{\ln\left(\frac{K1}{L\lambda}+1\right)} \quad \text{Eq.7}$$

Where; BT = effective at-sensor brightness temperature in Kelvin

$K1$ = calibration constant 1 (W/ (m^2 * sr * μm))

$K2$ = calibration constant 2 (W/ (m^2 * sr * μm))

$L\lambda$ = spectral radiance at the sensor's aperture (W/ (m^2 * sr * μm))

ln = natural logarithm

The temperature values estimated using Eq.9 were converted from Kelvin (K) to Celsius (°C) (a standard unit of measuring temperature) by subtracting 273.15.

Table 3: Thermal constants of Landsat images

Satellite	sensors	Categories	Band 6	Band 10	Band 11
Landsat 5	TM	K1	607.76		
		K2	1260.56		
Landsat 7	ETM+	K1	666.09		
		K2	1282.71		
Landsat 8	OLI/TIRS	K1		774.8853	480.8883
		K2		1321.0789	1201.1442

3.6.9. Normalized difference vegetation index

The Normalized Difference Vegetation Indices of the study area for the years 1987, 2003, and 2019 were calculated using Eq. 7. The vegetated areas reflect better in the near-infrared part of the spectrum (Roberts, et al., 2015). The normalized difference vegetation index is also used to infer general vegetation conditions and to determine the LST. The NDVI was obtained by using the red band (high absorption of radiation or low reflection) and the infrared band (low absorption of radiation or high reflection). Green leaves have a reflectance of 20% or less in the 0.5 to 0.7-micrometer range and about 60% in the 0.7 to 1.3 range (Farooq, et al., 2013). Therefore, NDVI values represent ratios ranging in value from −1.0 to 1.0. Accordingly, NDVI can be computed as

$$NDVI = \frac{\text{NIR}-\text{RED}}{NIR+RED} \qquad \text{Eq.8}$$

NDVI=Normalized Difference Vegetation Index

NIR= near-infrared band 4, RED= is the red band 3. The equation was used to calculate NDVI for the sensor TM, $ETM^{+,}$ and OLI. But in the case of Landsat 8, NIR is band 5 and the red band is a band 4 (Weng, et al., 2004).

3.6.10. Normalized difference built-up index

NDBI stands for Normalized Difference Built-up Index, In comparison to the other LULC surfaces, built-up lands have higher reflectance in the MIR wavelength range (1.55~ 1.75μm) than in the NIR wavelength range (0.76~ 0.90μm) (John & David, 1999). NDBI

is very useful for mapping the urban built-up areas and has been computed using the equation (8) expressed as follows;

$$NDBI = \frac{MIR-NIR}{MIR+NIR} \quad \text{Eq. 9}$$

Where *NIR* is near-infrared reflectance

MIR is middle infrared reflectance

NDBI values range from -1 to 1. The greater the NDBI is, the higher the proportion of built-up land is, and the larger areas of construction land have.

3.6.11. Land surface emissivity

To estimate LST the land surface emissivity (LSE (ε)) must be known because LSE is a proportional factor that scales blackbody radiance (Planck's law) to predict emitted radiance. In satellite images, pixels representing the land surface are usually mixed pixels, that is, they are a combination of surfaces-types such as water, vegetation, and soil. Therefore, the effective emissivity of a pixel can be calculated by summing up the contributions from those surface types because the emissivity value change from surface to surface. Though to estimate the emissivity from satellite thermal band data quite a lot of methods have been suggested, the NDVI threshold method was used in this study. Land surface emissivity was calculated via the following formula.

$$\varepsilon_\lambda = \varepsilon_v F_v + \varepsilon_s (1-F_v) + (1-\varepsilon_s)(1-\varepsilon_v) F\varepsilon_v \quad \text{Eq. 10}$$

Where εv and εs are the vegetation and soil emissivity, respectively, F = 0.55 shape factor considering different geometrical distributions, the fractional vegetation, Fv, was determined using the following equation (Meijun *et al.,* 2015).

$$Fv = \left(\frac{NDVI-NDVI_{min}}{NDVI_{max}-NDVI_{min}}\right)^2 \quad \text{Eq.11}$$

3.6.12. Statistical Analysis

To determine the correlations for each pixel, Pearson's correlation coefficients were calculated between the LST and the corresponding LULC indices values. Randomly, 368 points have been extracted from the image through ArcGIS software, finding the corresponding values of LST, NDVI, and NDBI for each year to estimate the relationship between them. The values were statistically analyzed for the creation of a model using

multiple linear regression with the help of Statistical Package for the Social Sciences (SPSS) version 20.

$$Y= \beta0+\beta1X1 +\beta2X2 +\beta3X3 +\ldots\ldots+\beta nXn \quad \text{Eq. (12)}$$

Where: Y= the dependent variable (LST)

β0 =Constant term of the model without the independent variables;

β1, β2...β10 = The Estimated influences of the specified independent variables;

X1, X2, to X10 = Independent variables which would be the predictor of the dependent variable

ANOVA and t-test were also applied to assess statistical significance between LST, NDVI, and NDBI. The relationship between land surface temperature and NDVI and NDBI can be determined by passing a multiple linear regression test. In the multiple linear regression test, the land surface temperature is taken as a dependent variable, while NDVI and NDBI are taken as independent variables for predicting the land surface temperature.

CHAPTER FOUR

4. RESULTS AND DISCUSSIONS

4.1. Results

4.1.1. LULC classes in 1987

The spatial extent of the 1987 LULC map after the Supervised Classification yielded land cover classes (Figures 10 and Table 4) with the high-density agriculture occupying the highest percentage of the area (13597.6 ha, 54.58%). The next LULC class with the highest area coverage was the forest (5087.52 ha, 20.42%) which was scattered around the North, South-West, South-East, and Western parts of the study area with very small patches in the southern part. Shrubland (3714.69 ha, 14.91%) was the next highest LULC class in the study area. Wetland comes next with (1389.65 ha, 5.58%) which was located around the south and South-Western part of Jimma city. This is followed by the settlement (1096.87 ha, 4.40%) located mainly around the center of the study area and waterbody (28.8 ha, 0.12%) was last and the least area coverage and concentrated in the eastern part of Jimma city.

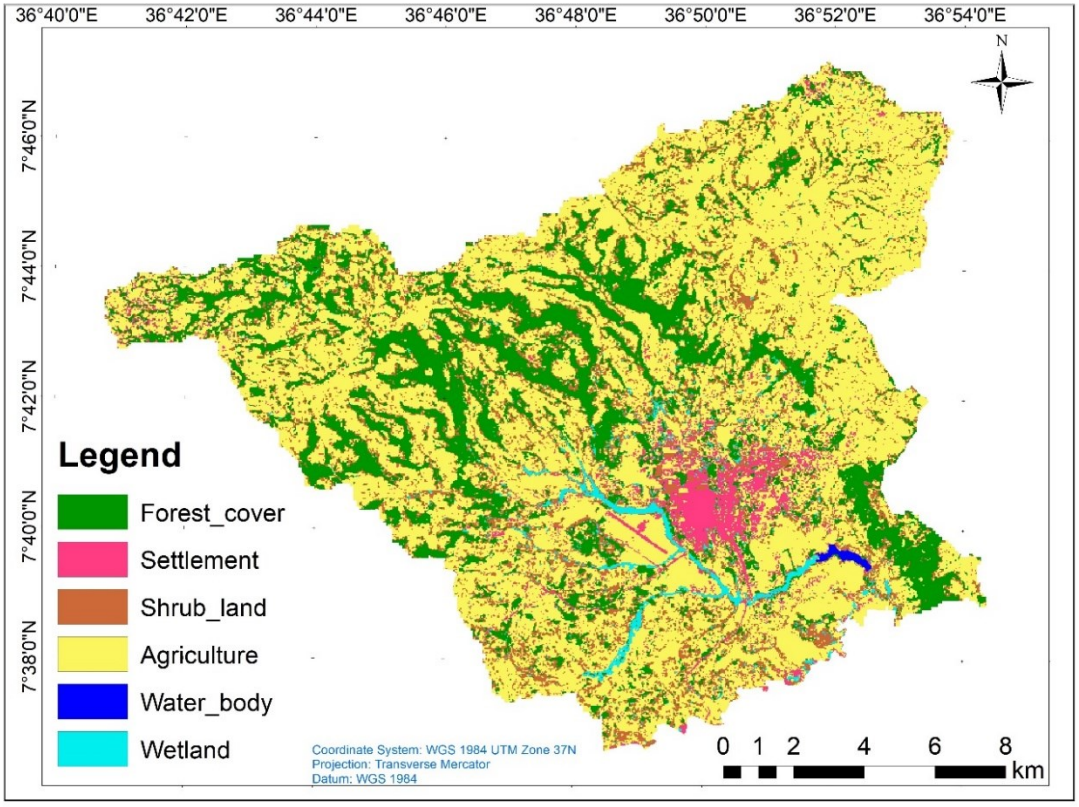

Figure 9: LULC map of the study area in 1987

Source: 1987 satellite image interpretation

Table 4: LULC classes and their area coverage in the three periods.

LULC classes	1987		2003		2019	
	ha	%	ha	%	ha	%
FC	5087.52	20.42	3293.54	13.22	3858.23	15.49
SET	1096.87	4.40	1881.04	7.55	3057.09	12.27
SH	3714.69	14.91	2615.4	10.50	1624.88	6.52
AG	13597.6	54.58	15836.1	63.56	15546.44	62.40
WB	28.8	0.12	16.56	0.07	0	0.00
WE	1389.65	5.58	1272.49	5.11	828.49	3.33
Total	24915.13		24915.13		24915.13	

Where: FC= Forest cover, SET= Settlement, SH= Shrub land, AG= Agriculture, WB= Water body and WE= Wetland.

4.1.2. LULC classes in 2003

The Supervised classification procedures applied to the 2003 Landsat ETM+ image yielded a land cover map with the high-density agriculture occupying the largest area coverage of (15836.1ha, 63.56%) as compared to other LULC classes (Figures 10 and Table 4). Forest covers an area of (3293.54ha, 13.22%) and is scattered around the North, South-West, South-East, and Western parts of the study area. Shrubland (3714.69 ha, 14.91%) was the third-highest LULC class in the study area. The settlement occupies an area of (1881.04ha, 7.55%) and is mainly concentrated at the center parts of the map. Wetland comes next with (1272.49ha, 5.11%) which was located around the southern part of Jimma city. Waterbody having (16.56ha, 0.07%) was the least area coverage and mainly concentrated in the eastern part of Jimma city.

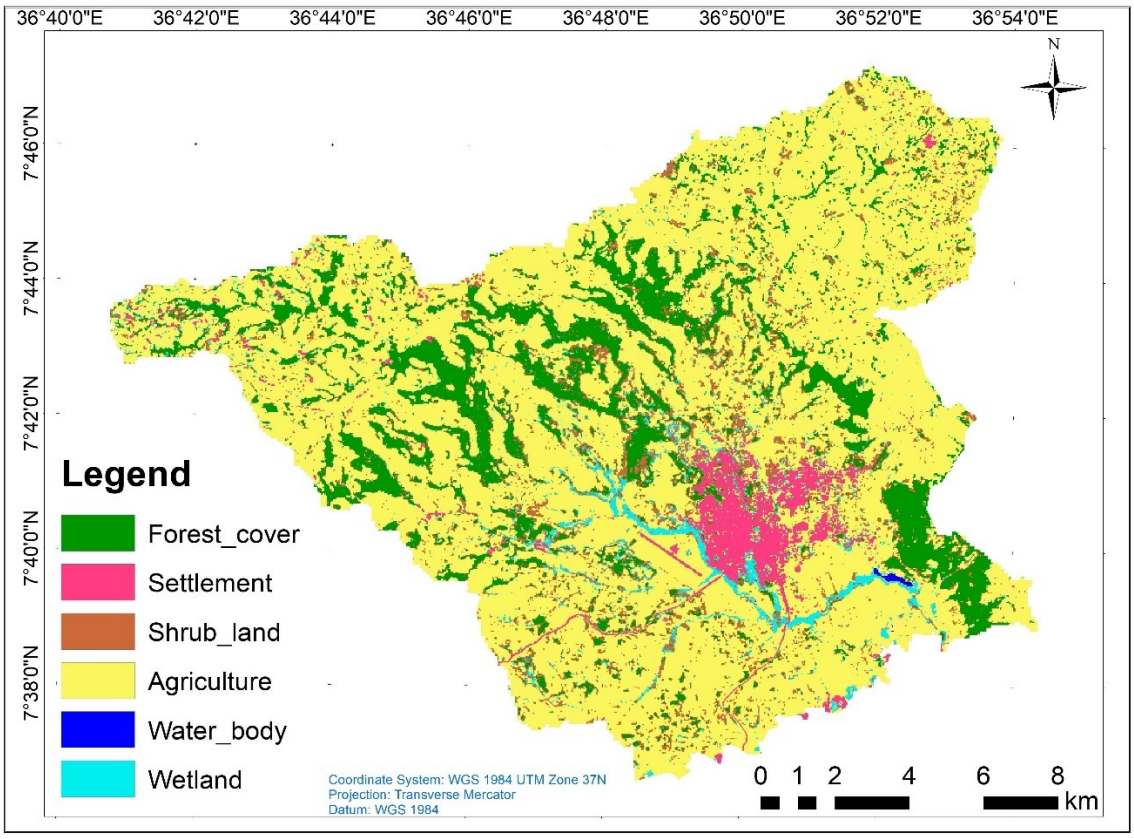

Figure 10: LULC map of the study area in 2003

Source: 2003 satellite image interpretation

4.1.3. LULC classes in 2019

The 2019 Landsat OLI/TIRS after classification procedures yielded a Land cover map with the high-density agriculture occupying an area of (15546.44ha, 62.40%). Forest covers an area of (3858.23ha, 15.49%) and mainly around the North, South-West, South-East, and Western parts of the study area with very small patches in the southern part. The settlement occupies an area of (3057.09ha, 12.27%). This was concentrated at the center of the map and small patches at the entire map. As (Figures 10 and Table 4) shows that shrubland, wetland, and waterbody have a dramatic decline and they account (1624.88ha, 6.52%), (828.49ha, 3.33%), and (0ha, 0.00%) respectively.

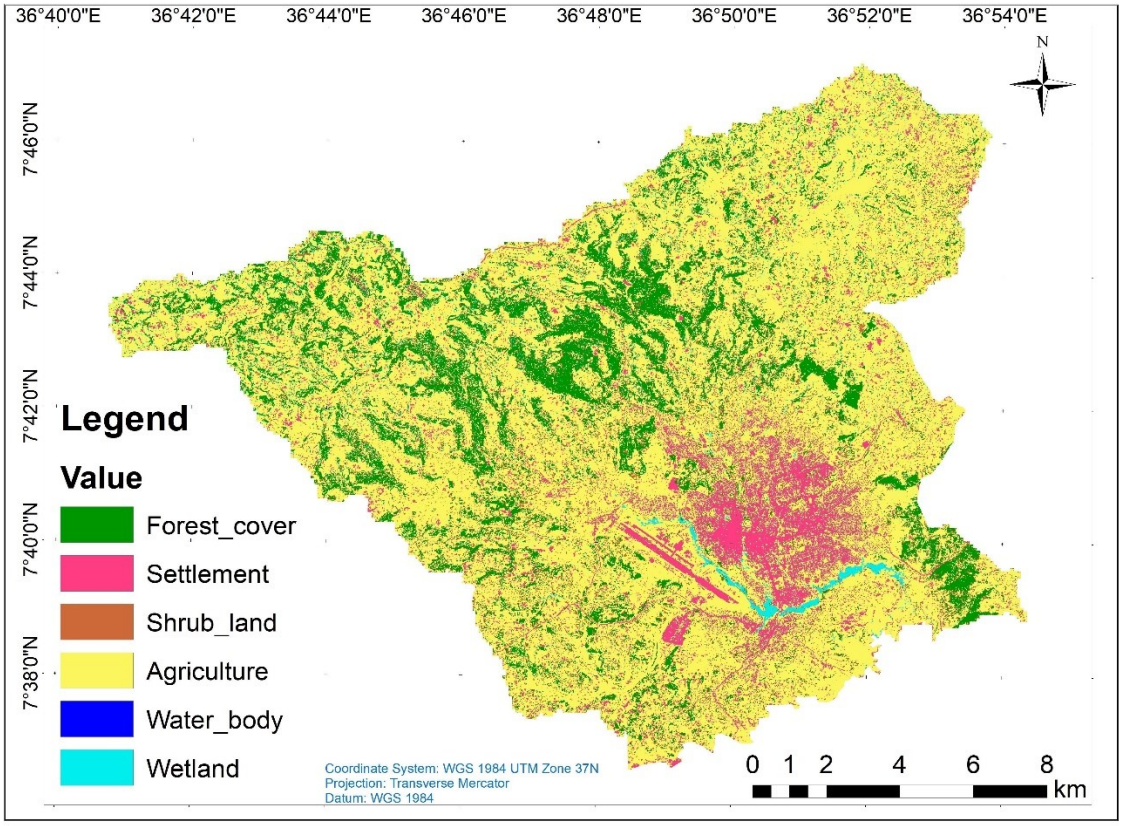

Figure 11: LULC map of the study area in 2019

Source: 2019 satellite image interpretation

4.1.4. LULC change between 1987 to 2003

The analysis of LULCC revealed that the agricultural land was 13597.6 ha (54.58%) of the study area in 1987 was increased to 15836.1ha (63.56%) in 2003 (Table 5). The net change in agricultural land was (14.14%, a positive rate of change). The settlement land was experienced the most positive change 41.69%, while waterbody experienced the most negative change (-73.91%). In contrary to settlement and agricultural land areas, forest cover, shrubland, and wetland areas were experienced negative change with (-54.47%), (-42.03), and (-9.21%) respectively (Figure 10).

Table 5: Extent of LULC change in 1987 and 2003 years.

LULC classes	1987		2003		Net-Change
	ha	%	ha	%	1987-2003 (%)
FC	5087.52	20.42	3293.54	13.22	-54.47
SET	1096.87	4.40	1881.04	7.55	41.69
SH	3714.69	14.91	2615.4	10.50	-42.03
AG	13597.6	54.58	15836.1	63.56	14.14
WB	28.8	0.12	16.56	0.07	-73.91
WE	1389.65	5.58	1272.49	5.11	-9.21
Total	24915.13		24915.13		

Where: FC= Forest cover, SET= Settlement, SH= Shrub land, AG= Agriculture, WB= Water body and WE= Wetland.

4.1.5. LULC change between 2003 to 2019

When analyzing the 2003 LULC classification with the 2019 LULC classification, the forest cover class shows increasing in the study area from 2003 to 2019 (Table 6). The increment of forest LULC was a direct reflection of the government policy of the millennium afforestation program to enhance the forest coverage of the country. The settlement land cover class shows a remarkable increase between 2003 and 2019, which has been increased in size from 1881.04 ha in 2003 to 3057.09 ha in 2019 with a net change (38.47%, positive rate of change), while the water bodies were experiencing an extremely decreased from 16.65 ha in 2003 to 0 ha in 2019. The increment of settlement area over

the study period was associated with rapid population growth, migration of people from a neighboring city, and unable to compete for the land lease price. These results are consistent with (Mosammam *et al.,* 2017) who reported that the rapid urban population is a key challenge of the twenty-first century. Two land cover classes namely settlement and agricultural land show an increasing trend throughout the study periods (Table 6 and Figure 10).

Table 6: Extent of LULC change in 2003 and 2019 years.

LULC classes	2003		2019		Net-Change
	ha	%	ha	%	2003-2019 (%)
FC	3293.54	13.22	3858.23	15.49	14.64
SET	1881.04	7.55	3057.09	12.27	38.47
SH	2615.4	10.50	1624.88	6.52	-60.96
AG	15836.1	63.56	15546.44	62.40	-1.86
WB	16.56	0.07	0	0.00	0.00
WE	1272.49	5.11	828.49	3.33	-53.59
Total	24915.13		24915.13		

Where: FC= Forest cover, SET= Settlement, SH= Shrub land, AG= Agriculture, WB= Water body and WE= Wetland.

4.1.6. LULC change between 1987 to 2019

Generally, the trend analysis of the study area reveals a change in the LULC types over the three study periods (Table 7 and Figure 10). The settlement experienced the most positive change 64.12%, while shrubland experienced the most negative change (-128.61%) during the years 1987 to 2019. The settlement land increased from 1987 to 2019 covering an area of 1096.87ha (4.40%) in the year 1987 and 1881.04 ha (7.55%) in the year 2003 and 16 years later this land cover class increased to 3057.09 ha (12.27%) in the year 2019. The study conducted by (Dube, 2013) also found comparable results with increased settlement areas due to rapid, unstructured, and unplanned development. The increasing trends are also observed in agricultural land. However, the shrubland and forest cover that occupies

over 3714.69 ha (14.91%) and 5087.52 ha (20.426%) in 1987 respectively, decreased to 1624.88 ha (6.52%) and 3858.23 ha (15.49%) in 2019 respectively.

Table 7: Extent of LULC change in 1987 and 2019 years.

LULC classes	1987		2019		Net-Change
	ha	%	ha	%	1987-2019 (%)
FC	5087.52	20.42	3858.23	15.49	-31.86
SET	1096.87	4.40	3057.09	12.27	64.12
SH	3714.69	14.91	1624.88	6.52	-128.61
AG	13597.6	54.58	15546.44	62.40	12.54
WB	28.8	0.12	0	0.00	0.00
WE	1389.65	5.58	828.49	3.33	-67.73
Total	24915.13		24915.13		

Where: FC= Forest cover, SET= Settlement, SH= Shrub land, AG= Agriculture, WB= Water body and WE= Wetland.

The declining trend of the shrubland and forest cover was due to increasing land requirements for house construction and arable land, which arising from (rapid population growth, density, and internal migration), urbanization, and uncontrolled response by the government (Deribew & Dalacho, 2019), which enhances the problem of informal house constructions. These findings are supported by (Abebe *et al.,* 2019), who reported urban informality, is the outcome of either the population who lives in substandard living conditions or a housing deficit. It is observed that the water body has decreased from 28.8 ha (0.12%) in the year 1987 to 16.56 ha (0.07%) in the year 2003, and the decreasing trend of water body was continued throughout the study period and decreased to 0 ha (0%) by the year 2019. The wetland of the study area also shows a decreasing trend from 1987 to 2019 covering a total area of 1389.65 ha (5.58%) in the year 1987 and 828.49 ha (3.33%) in 2019. The decreasing trend in both water bodies and wetland is because the deposition of sediment in the water bodies and wetland resulted, silt from farmland, sludge from infrastructure built in the city, and housing. In agreement with the finding of this study (Abrha *et al.,* 2015) also reported the reduction of water bodies and wetland between 1984

and 2007 were corresponding to the drastic consequences of ever-increasing demand for residential and institutional building construction spaces in Jimma city.

4.1.7. Land use land cover change matrix

To acquire changes of the six LULC classes over the study period (1987–2019), the change matrix was conducted through cross-tabulation to investigate the trend, net change, and percent change between 1987 and 2003, 2003 and 2019, and for the overall study period 1987 and 2019.

Table 8 shows a summary of the major LULC conversions that have been taken place from 1987 to 2003 within the study area. The diagonal of the table shows the LULC proportions that remain unchanged from 1987 to 2003, a total area of 19,130.5 ha representing 76.78% of the study area. From the table, forest cover in 1987 was converted into agricultural land, shrubland, and settlement in 2003. The major forest cover transformation made by the expansion of agricultural land was (22.05%) and shrubland was (12.70%). In contrary to this, (0.99%) Forest cover was gained from shrubland in 2003. Shrubland also changed to agricultural land, wetland, and settlement in 2003. Furthermore, the water body was transformed into wetland, agriculture, shrubland, and settlement. Similarly, the wetland was changed to agriculture, shrubland, and settlement in 2003. Details about the LULC transformation matrix from 1987-2003 are illustrated in Table 8.

Table 8: LULC changes matrix of the Jimma city and its surrounding from 1987 to 2003 (ha)

		LULC of 2003													
	LULC	FC		SET		SH		AG		WB		WE		class total	
	Class	ha	%	ha	%	ha	%	ha	%	ha	%	ha	%	ha	%
LULC of 1987	FC	3199.06	62.88	120.29	2.36	646.05	12.70	1121.75	22.05	0	0.00	0.37	0.01	5087.52	100
	SET	0.64	0.06	1030.32	93.93	21.37	1.95	44.54	4.06	0	0.00	0	0.00	1096.87	100
	SH	36.81	0.99	133.77	3.60	1766.1	47.54	1595.87	42.96	0	0.00	182.14	4.90	3714.69	100
	AG	51.94	0.38	582.04	4.28	94.09	0.69	12452.92	91.58	0	0.00	416.61	3.06	13597.6	100
	WB	0	0.00	0.45	1.56	0.54	1.88	3.42	11.88	16.56	57.50	7.83	27.19	28.8	100
	WE	5.09	0.37	14.17	1.02	87.25	6.28	617.6	44.44	0	0.00	665.54	47.89	1389.65	100
	class total	3293.54	13.22	1881.04	7.55	2615.4	10.50	15836.1	63.56	16.56	0.07	1272.49	5.11	24915.13	100

Where: FC= Forest cover, SET= Settlement, SH= Shrub land, AG= Agriculture, WB= Water body and WE= Wetland.

As Table 9 shows, from the total area of forest cover in 2003, 785.01 ha (23.83%), 254.32 ha (7.72%), and 48.24 ha (1.46%) were converted to agriculture, shrubland, and settlement in 2019, respectively. On contrary, forest cover was gained from shrubland 845.79 ha and agricultural land 804.97 ha in 2019. During 2003-2019, shrubland was also converted into agriculture and settlement. The conversion of agricultural land to other LULC classes such as settlement (6.38%), shrubland (4.32%), and wetland (2.44%) after sixteen years. Waterbody also changed into wetland (55.31%), agriculture (42.81%), shrubland (1.03%), and settlement (0.87%) in the year 2019. Similarly, the wetland was transformed into agriculture, shrubland, and settlement. Table 9 present the detailed information of LULC transformation from 2003 to 2019.

Table 9: LULC changes matrix of the Jimma city and its surrounding from 2003 to 2019 (ha)

		LULC of 2019													
	LULC	FC		SET		SH		AG		WB		WE		class total	
	Class	ha	%	ha	%	ha	%	ha	%	ha	%	ha	%	ha	%
LULC of 2003	FC	2205.94	66.98	48.24	1.46	254.32	7.72	785.01	23.83	0	0.00	0.03	0.00	3293.54	100
	SET	1.5	0.08	1831.21	97.35	9.32	0.50	39.01	2.07	0	0.00	0	0.00	1881.04	100
	SH	845.79	32.34	113.41	4.34	568.79	21.75	1081.9	41.37	0	0.00	5.51	0.21	2615.4	100
	AG	804.97	5.08	1010.27	6.38	683.84	4.32	12950.89	81.78	0	0.00	386.13	2.44	15836.1	100
	WB	0	0.00	0.14	0.85	0.17	1.03	7.09	42.81	0	0.00	9.16	55.31	16.56	100
	WE	0.03	0.00	53.82	4.23	108.44	8.52	682.54	53.64	0	0.00	427.66	33.61	1272.49	100
	class total	3858.23	15.49	3057.09	12.27	1624.88	6.52	15546.44	62.40	0	0.00	828.49	3.33	24915.13	100

Where: FC= Forest cover, SET= Settlement, SH= Shrub land, AG= Agriculture, WB= Water body and WE= Wetland.

While considering the whole range of time under consideration, the reduction in the area covered by forest, shrubland, water body, and wetland were observed. Image differencing of the two different times, 1987, and 2019 indicated that forest cover was reduced from 5087.52 ha to 3858.53 ha (1229.29 ha) representing 31.86% of the area. The conversion of forest cover to other LULC classes such as agriculture (39.15%), shrubland (9.11%), and settlement (3.50%). On contrary, forest cover was gained from shrubland (13.89%) and agricultural land (6.43%). Other LULC conversions are shrubland to agricultural land (64.85%), settlement (6.96%), and wetland (2.03%). Agricultural land was also transformed into settlement (10.85%) and shrubland (4.96%). Furthermore, waterbody was changed to wetland (54.51%), agricultural land (42.95%), and shrubland (2.05%). Similarly, the wetland was also changed to agriculture (45.79%), settlement (5.78%), and shrubland (1.71%). The LULCC matrix of the study area from 1987 to 2019 is illustrated in (Table 10).

Table 10: LULC changes matrix of the Jimma city and its surrounding from 1987 to 2019 (ha)

		LULC of 2019													
	LULC	FC		SET		SH		AG		WB		WE		class total	
	Class	ha	%	ha	%	ha	%	ha	%	ha	%	ha	%	ha	%
LULC of 1987	FC	2453.73	48.23	178.16	3.50	463.46	9.11	1991.54	39.15	0	0.00	0.63	0.01	5087.52	100
	SET	7.5	0.68	1065.25	97.12	6.45	0.59	17.67	1.61	0	0.00	0	0.00	1096.87	100
	SH	515.84	13.89	258.49	6.96	455.72	12.27	2409.1	64.85	0	0.00	75.54	2.03	3714.69	100
	AG	874.51	6.43	1474.79	10.85	674.95	4.96	10479.11	77.07	0	0.00	94.24	0.69	13597.6	100
	WB	0	0.00	0.14	0.49	0.59	2.05	12.37	42.95	0	0.00	15.7	54.51	28.8	100
	WE	6.95	0.50	80.26	5.78	23.71	1.71	636.35	45.79	0	0.00	642.38	46.23	1389.65	100
	class total	3858.53	15.49	3057.09	12.27	1624.88	6.52	15546.14	62.4	0	0.00	828.49	3.33	24915.13	100

Where: FC= Forest cover, SET= Settlement, SH= Shrub land, AG= Agriculture, WB= Water body and WE= Wetland.

4.1.8. Accuracy Assessment

The accuracy evaluation of LULC for the year 2019 was validated using a ground-truthing assessment of 210 sample GPS points taken from the study area, resulting in an overall accuracy of 89.14 % (Table 11). For the year 2019, the classification Kappa statistics value was 0.8643. The confusion matrix was calculated using Google Earth and KII to validate the accuracy for the years 1987 and 2003, yielding overall accuracy of 81.90 % and 83.81 %, respectively. For the years 1987 and 2003, the overall LULC classification Kappa statistics were 0.7829 and 0.8057, respectively.

Table 11: Confusion matrix of the year 2019 LULC supervised classification

Class name	1987		2003		2019	
	Producers Accuracy	Users Accuracy	Producers Accuracy	Users Accuracy	Producers Accuracy	Users Accuracy
FC	85.71%	96.77%	97.14%	94.44%	91.43%	96.97%
SET	71.43%	96.15%	94.29%	89.19%	88.57%	96.88%
SH	82.86%	61.70%	82.86%	96.67%	85.71%	90.91%
AG	91.43%	80.00%	91.43%	74.42%	91.43%	80.00%
WB	62.86%	95.65%	51.43%	94.74%	0	0
WE	97.14%	79.07%	85.71%	66.67%	88.57%	83.78%
Overall Accuracy	81.90%		83.81%		89.14%	
(K^)	0.7829		0.8057		0.8643	

Where: FC= Forest cover, SET= Settlement, SH= Shrub land, AG= Agriculture, WB= Water body and WE= Wetland.

4.1.9. Normalized difference vegetation index

In this study, it has been observed that the vegetation cover was very high in 1987 than in 2003 with maximum NDVI values of 0.61 and 0.48 respectively. This indicates that there was high healthy vegetation cover in 1987 than in 2003. Urban expansion and depletion of vegetation cover in 2003 were responsible for the decline of NDVI values. In 2019, vegetation cover was slightly increased and this made the NDVI value increase from 0.48 to 0.52 (Table 12).

As indicated in Figure 11 vegetation cover has decreased and the non-vegetated area has been increasing gradually over the study period. However, in 2019 plantation of (some trees and cash crops area has slightly increased due to the plantation program both in rural and urban areas). Settlement and agricultural land have low NDVI values. This is because of the dry nature of those surfaces and their high thermal emittance property. So, this indicates that there was an indirect relationship between NDVI and LST. Sun *et al.,* (2012) and Yue *et al.,* (2007) revealed that LST has inversely related to NDVI.

Table 12: Normalized difference vegetation index results in 1987, 2003 and 2019

	1987				2003				2019			
Class			Mean				Mean				Mean	
Name	Min	Max	NDVI	STD	Min	Max	NDVI	STD	Min	Max	NDVI	STD
FC	0.13	0.61	0.39	0.05	0.09	0.48	0.32	0.05	0.01	0.52	0.29	0.06
SET	-0.07	0.46	0.21	0.07	-0.32	0.30	0.00	0.10	-0.42	0.40	0.18	0.06
SH	0.26	0.42	0.33	0.03	-0.01	0.37	0.16	0.06	0.10	0.44	0.30	0.04
AG	0.01	0.45	0.24	0.05	-0.33	0.36	0.01	0.09	-0.03	0.45	0.26	0.05
WB	-0.22	0.14	-0.08	0.09	-0.04	0.10	-0.12	0.12	0.00	0.00	0.00	0.00
WE	0.28	0.59	0.40	0.05	0.12	0.38	0.23	0.04	0.05	0.47	0.32	0.05

Where: FC= Forest cover, SET= Settlement, SH= Shrub land, AG= Agriculture, WB= Water body, WE= Wetland, MIN = Minimum, MAX = Maximum, STD = Standard deviation.

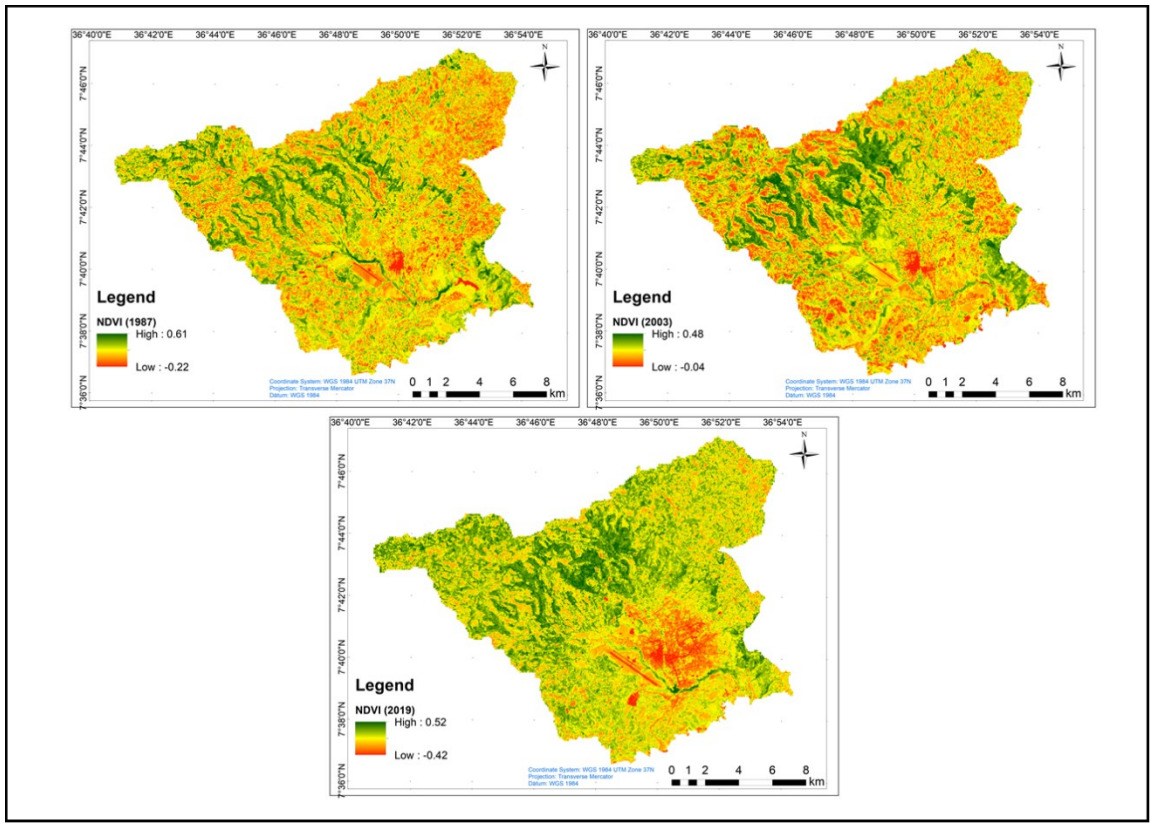

Figure 12: NDVI map of Jimma city and its surrounding in 1987, 2003 & 2019

4.1.10. Normalized difference built-up index

High NDBI values were concentrated around agricultural land and in the city area of Jimma. The build-up areas and bare land reflect more SWIR than NIR. In the case of a green surface, a reflection of NIR is higher than the SWIR spectrum (Zha *et al.,* 2003). Hence the lower value of NDBI represents vegetation whereas the higher value represents settlement and agricultural areas. In agreement with the finding of this research, a study conducted by Xiong *et al.,* (2012) found that high-temperature anomalies are closely associated with built-up land, densely populated zones, and heavily industrialized districts. Figure 12 indicated that the NDBI values were increased around Jimma city.

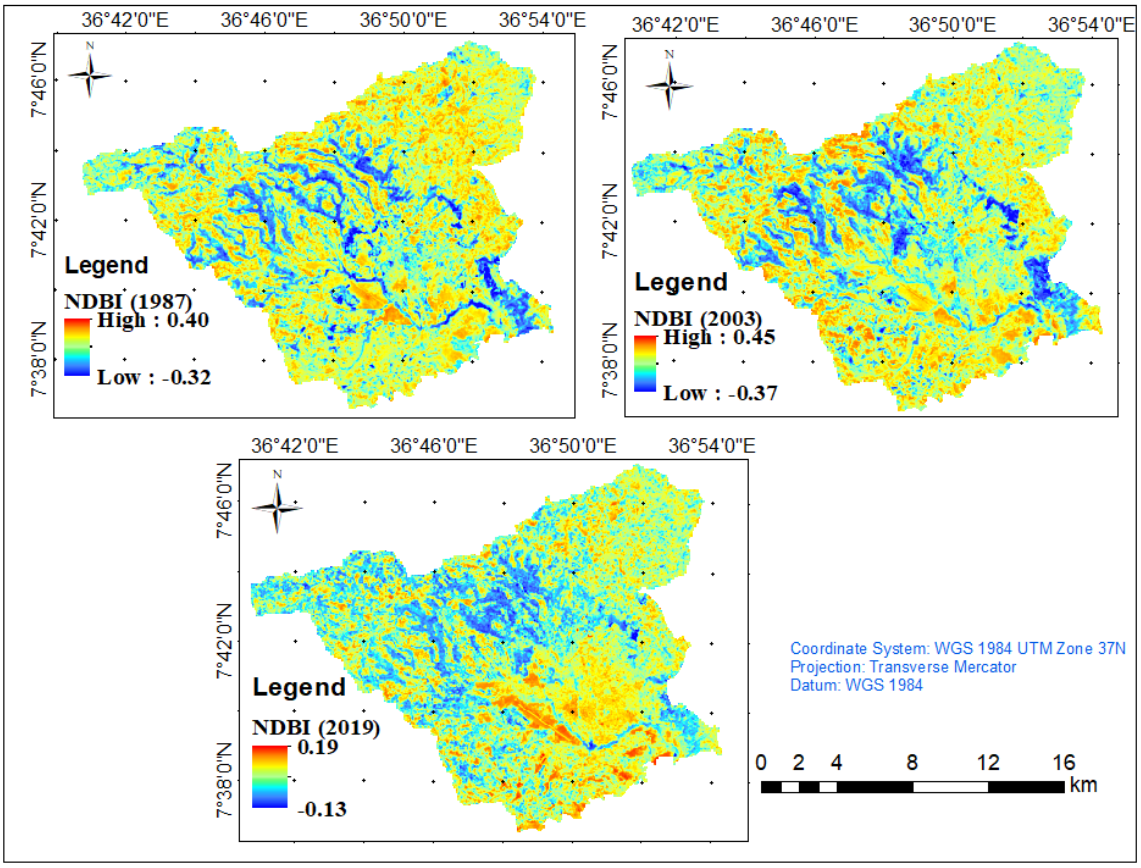

Figure 13: NDBI map of Jimma city and its surrounding in 1987, 2003 & 2019

4.1.11. The relationship of LST and LULC

Table 13 summarizes the LST and NDVI regressions for each LULC, with R^2 indicating the regression's determination coefficient. Forest cover, shrubland, and agricultural land had greater NDVI-to-LST coefficients. In wetland, water bodies, and settlement land, however, the LST and NDVI coefficients were small during the study period. Overall, the minimum temperature was found in the range of 12.36˚C in forest cover in 1987 to 21.53˚C in a settlement in 2019 while, the maximum temperature was recorded in the range of 19.28˚C in waterbody in 1987 to 33.68˚C in agricultural land in 2019 (Figure 13 and Table 14). In addition, the mean temperature was seen at around 16˚C in the waterbody in 1987 to 28˚C in the settlement in 2003. The lowest value for minimum 12.36˚C, maximum 19.28˚C, and mean 16.22˚C temperature can be found in the year 1987. Meanwhile, the highest value for the minimum temperature was occurred in 2019 (21.51˚C) in the settlement, and the highest value of the maximum and mean temperature was occurred in

2003 (35.92°C and 28.16°C) in a settlement. The lowest rate of increase in LST is found under forest cover.

Table 13: Linear regression equations between LST and LULC

years	LULC	Regression	R^2
1987	FC	LST = -7.3477x NDVI + 16.723	0.8919
	SET	LST = -0.2627x NDVI + 19.582	0.0001
	SH	LST = -13.858x NDVI + 23.007	0.1554
	AG	LST = -7.2137x NDVI + 22.259	0.0414
	WB	LST = -3.8903x NDVI + 15.705	0.0103
	WE	LST = -6.4279x NDVI + 21.188	0.0119
2003	FC	LST = -12.523x NDVI + 27.05	0.3129
	SET	LST = -1.6249x NDVI + 22.533	0.0049
	SH	LST = -12.685x NDVI + 28.318	0.2894
	AG	LST = -12.917x NDVI + 27.231	0.1941
	WB	LST = -1.3986x NDVI + 20.666	0.0256
	WE	LST = -13.969x NDVI + 27.883	0.1837
2019	FC	LST = -25.305x NDVI + 33.041	0.8043
	SET	LST = -20.946x NDVI + 30.51	0.335
	SH	LST = -20.519x NDVI + 31.032	0.4441
	AG	LST = -21.849x NDVI + 31.193	0.4342
	WB	- -	-
	WE	LST = -20.648x NDVI + 30.719	0.3618

Table 14: The mean LST and its standard deviation in different LULC types, which were calculated through GIS spatial partition statistics.

	1987				2003				2019			
Class Name	Min	Max	Mean LST	STD	Min	Max	Mean LST	STD	Min	Max	Mean LST	STD
FC	12.36	25.40	17.29	1.90	17.09	29.31	22.11	1.46	20.11	32.10	23.57	1.39
SET	13.78	27.51	20.53	1.83	17.62	35.92	28.16	2.12	21.51	33.60	26.79	1.64
SH	13.78	24.54	19.15	1.55	18.15	32.18	25.14	1.59	21.02	30.63	24.60	1.30
AG	13.78	26.67	19.59	1.84	16.55	34.99	26.85	2.23	21.03	33.68	25.82	1.63
WB	15.64	19.28	16.22	0.55	19.21	29.30	21.61	1.10	-	-	-	-
WE	14.25	24.11	17.50	1.65	20.26	32.18	24.68	1.43	21.02	32.29	25.04	1.56

Where: FC= Forest cover, SET= Settlement, SH= Shrub land, AG= Agriculture, WB= Water body, WE= Wetland, MIN = Minimum, MAX = Maximum, STD = Standard deviation.

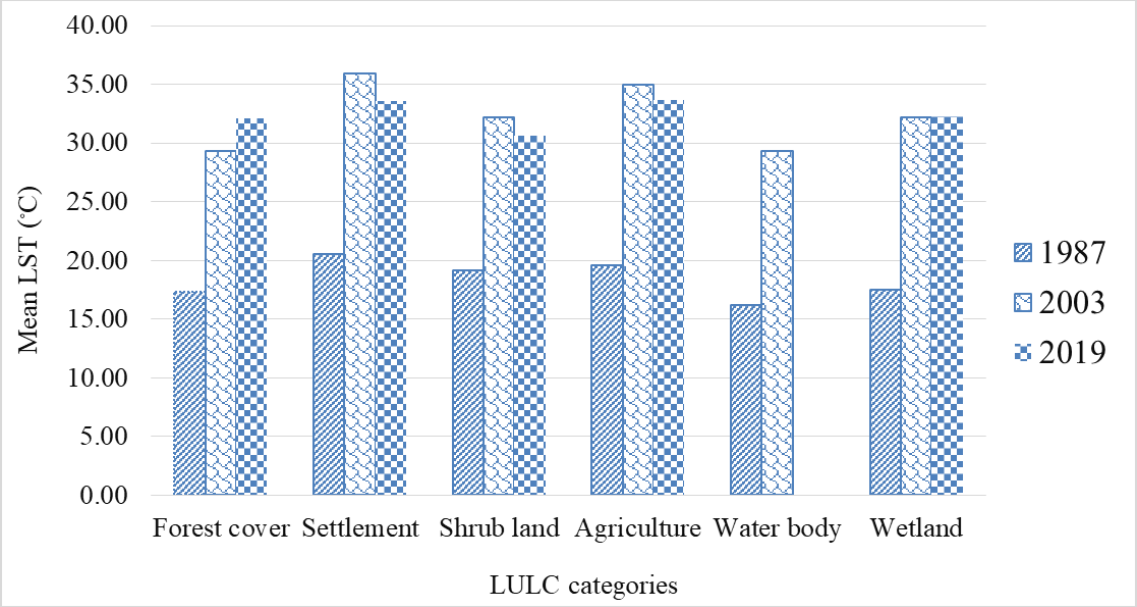

Figure 14: The mean LST in different LULC types.

To understand the relationship that exists between the land cover types and the LST, the mean value of the LST for 2019 and the corresponding percentage proportion of NDVI was investigated for each land cover type through correlation analysis (Table 15). The results show that there is a strong negative correlation between the mean LST and the percentage proportion of the vegetated areas of the Forest cover, shrubland, and wetland. This means that as the proportion of vegetated surfaces increases, the mean LST decreases. These results were found to be highly significant at $P < 0.01$. In contrast, other results revealed a strong positive correlation between the mean LST and percentage proportion of non-vegetated areas such as settlement and agricultural land implies that as the percentage proportion of non-vegetated areas increases, the mean LST increases. The results were also highly significant at $P < 0.01$. Because of this relationship between LST and NDVI, changes in LULC have an indirect impact on surface temperatures through NDVI. 1Ho is rejected and 1H1 is accepted based on the significant value of the p test results. This suggests that LULC has a significant impact on the temperature of the land surface.

Table 15: Pearson's correlations between LST and each indices of LULC 2019

Variables	LST	FC	SET	SH	AG	WE
LST	1	-.449**	.868**	-.660**	.674**	-.643**
FC	-.449**	1	.135	.268*	.235	.455*
SET	.868**	.135	1	-.632**	.305	-.682**
SH	-.660**	.268*	-.632**	1	.115	.393
AG	.674**	.235	.305	.115	1	-.164*
WE	-.643**	.455*	-.682**	.393	-.164*	1

**. Correlation is significant at the 0.01 level (2-tailed).

*. Correlation is significant at the 0.05 level (2-tailed).

Where: FC= Forest cover, SET= Settlement, SH= Shrub land, AG= Agriculture, WB= Water body and WE= Wetland.

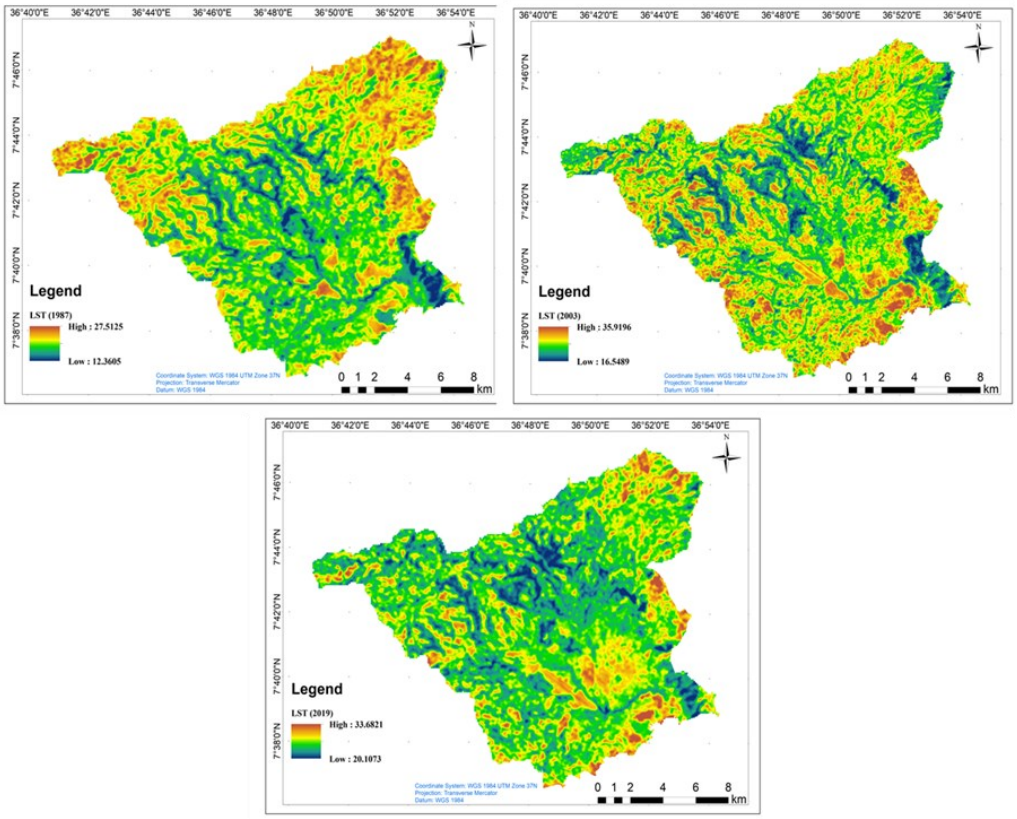

Figure 15: LST map of Jimma city and its surrounding in 1987, 2003 & 2019

Figure 14 and Table 14 shows that high surface temperature was observed in settlement land and agricultural land whereas the low surface temperature in green vegetative and wetland areas. Therefore, with the expansion of the vegetated area, the LST value adversely decreases and the expansion of non- evaporating surface brought an increase in LST. An increase in density of settlement, reduction in open space and green cover, increase in built-up space improves the LST of the urban area (Lilly & Devadas, 2009). With the rapid growth and expansion of the urban area, the propensity for the conversion of LULC into a built-up area and dwelling unit (non-evaporating surface) becomes high. Thus, such surfaces have a high probability of showing a greater value of LST.

Table 16: Model summary of LST and each indices of LULC 2019

Model	R	R Square	Adjusted R Square	Std. Error of the Estimate
1	.911[a]	.829	.749	.15960

a. Predictors: (Constant),

b. Dependent Variable:

For the full regression model, R^2 of 0.829 indicated the explanatory power of the model (Table 16). Thus, 82% of the variation in the dependent variables was explained by the regression. The significant value of 0.000 is lesser than the alpha value of 0.05, which indicates that the independent variables are statistically significant for the prediction of the dependent variable (Table 17), $F(7, 15) = 10.396$, $p < 0.05$ which means the adopted regression model is a good fit of the data.

Table 17: ANOVA of LST and each indices of LULC 2019

Model		Sum of Squares	df	Mean Square	F	Sig.
1	Regression	1.854	7	.265	10.396	.000[b]
	Residual	.382	15	.025		
	Total	2.236	22			

a. Dependent Variable: LST_2019

b. Predictors: (Constant),

From Figure 15 Forest cover type was located in the right lower corner of the diagram, shrubland, and wetland areas were located in the center of the diagram (medium values for both parameters, NDVI and LST), while the settlement and agricultural land areas were located at the upper left corner of the diagram. In other words: the NDVI confirms the cluster structure of land cover types derived from surface temperatures

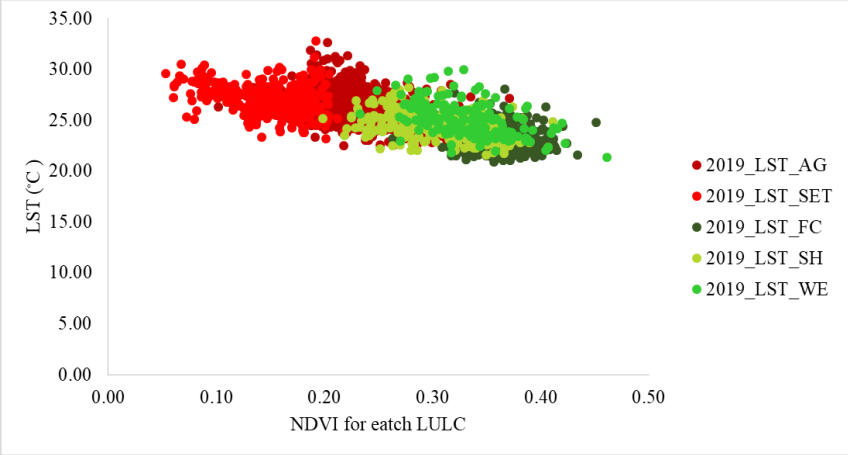

Figure 16: Scatterplot of LST vs. NDVI (2019).

4.1.12. Multiple correlation matrix analysis of LST, NDVI, and NDBI

The analyzed Landsat images of 1987 and 2019 indicated that LST had a positive relationship with NDBI and an inverse relationship with NDVI.

Table 18: Model Summary of LST and NDVI and NDBI for 1987, 2003 & 2019

Years	Model	R	R Square	Adjusted R Square	Std. Error of the Estimate
1987	1	.831[a]	.691	.689	1.26820
2003	1	.880[a]	.774	.773	1.34958
2019	1	.885[a]	.784	.782	1.05233

a. Predictors: (Constant), NDBI, NDVI

From the processing results obtained summary (Table 18) which shows the values of determination (R^2) to determine the percentage contribution of the influence of the independent variables to the dependent variable and the values of R (multiple correlation coefficients) which are considered as a measure of the worth of the prediction of the

dependent variables. The R-value of 0.831, 0.880, and 0.885 for the years 1987, 2003, and 2019 respectively indicate a good level of prediction. The coefficient of determination was represented by R^2 which shows the proportion of variance in the dependent variable that can be explained by the independent variables. The R square values were 0.691, 0.774, and 0.784 for the years 1987, 2003, and 2019 respectively; therefore, above 69.1%, 77.4%, and 78.4% of the variation in the land surface temperature (dependent variable) was explained by NDVI and NDBI (independent variables) shown in Table 18.

Simultaneously it can be seen from the F-ratio in the ANOVA test results. (Table 19) shows that the independent variables highly statistically significantly predict the dependent variable, F (2, 366) =326.166, p (0.000), (2, 366) =416.379, p (0.000) and (2, 366) =238.771, p (0.000) for the year 1987, 2003 and 2019 respectively (i.e., the regression model is a good fit of the data). Table 19 shows the analysis of variance, which shows the overall regression model is a good fit for the given data.

Table 19: ANOVA of LST and NDVI and NDBI for 1987, 2003 & 2019

year	Model		Sum of Squares	df	Mean Square	F	Sig.
1987	1	Regression	1049.170	2	524.585	326.166	.000[b]
		Residual	468.652	366	1.608		
		Total	1517.822	368			
2003	1	Regression	1247.080	2	623.540	416.379	.000[b]
		Residual	448.096	366	1.498		
		Total	1695.176	368			
2019	1	Regression	745.220	2	282.610	238.771	.000[b]
		Residual	253.199	366	1.184		
		Total	998.419	368			

a. Dependent Variable: LST

b. Predictors: (Constant), NDBI, NDVI

Table 20 and Figures 16a-c show the unstandardized coefficient (B), which tells the relationship between the land surface temperature and other independent variables. There was a strong negative correlation (B = -0.078) between LST and NDVI of the year 1987 and highly statistically significant (ρ = 0.000). NDVI of the year 2003 shows a negative

correlation (B = -0.048) with LST and is statistically significant (ρ= 0.000). There was also a strong negative correlation (B= -0.022) between LST and NDVI of the year 2019 and statistically significant (ρ= 0.000). Malik *et al.,* (2019), Balew (2018), and Haylemariya (2018) revealed that LST has inversely related to NDVI. The negative value of NDVI implies that the land surface temperature increase, with decreases in vegetation, so LST is negatively related to NDVI. According to KII, Jimma city's forest cover has been converted to built-up other infrastructure. Other LULC, such as wetland, shrubland, and forest land, were also converted to agricultural land and settlement. Transformation of vegetation areas, expansion of settlement land, and agricultural land were responsible for the increase of LST in the study area. If the deforestation and cut of urban trees are not stopped, then this situation will continue to be worse day by day.

Table 20: Coefficients of LST and NDVI and NDBI for 1987, 2003 & 2019

year	Model		Unstandardized Coefficients		Standardized Coefficients			95.0% Confidence Interval for B	
			B	Std. Error	Beta	t	Sig.	Lower Bound	Upper Bound
1987	1	(Constant)	19.641	.659		29.796	.000	18.345	20.937
		NDVI	-.078	1.793	-.025	-3.741	.000	-10.234	-3.182
		NDBI	.572	1.519	.038	7.618	.000	8.586	14.558
2003	1	(Constant)	25.267	.369		68.546	.000	24.542	25.991
		NDVI	-.048	1.371	-.036	-5.459	.000	-10.176	-4.787
		NDBI	.612	1.165	.060	9.970	.000	9.321	13.902
2019	1	(Constant)	28.933	.390		74.097	.000	28.165	29.701
		NDVI	-.022	1.718	-.001	-5.880	.000	-13.481	-6.724
		NDBI	.759	1.340	.049	8.337	.000	8.534	13.802

a. Dependent Variable: LST

The linear regression between LST and NDBI and the trend analysis in Figure16a-c and Table 20 represents the rise of LST with the increase of NDBI value over time. The value of the coefficient of determination, R^2= 0.754 in 1987 (Figure17a) describes the strong responsive relationship between LST and NDBI. The transformation of other land cover types in buildup areas has influenced the relationship in the year 2019. The value of R^2= 0.739 in the year 2019 (Figure 17c) indicates the strongly significant positive relationship

between LST and NDBI. The coefficient of determination in Figures 17a,b,c suggests that the increase of settlement area is responsible for the increase of surface temperature in the study area during the study period. NDBI was strongly positively correlated (B = 0. 572, B= 0.612 and B= 0.759) to the LST and indicate highly statistically significant (ρ = 0.000) for the year 1987, 2003 and 2019 respectively. The positive B value of NDBI indicates that an increase in settlement land will increase the temperature which indicates that LST is positively related to NDBI.

Table 20 also show 1987 NDVI (t = -3.741, p < 0.05), 1987 NDBI (t = 9.970, p < 0.05), 2003 NDVI (t = -5.459, p < 0.05), 2003 NDBI (t = 7.618, p < 0.05), 2019 NDVI (t = -5.880, p < 0.05), 2019 NDBI (t = 8.337, p < 0.05) are significant predictors of land surface temperature.

Based on the results of the t-test, the significance value of each variable was less than 0.05 then the hypothesis 2H1 was accepted. Therefore, the NDVI and the NDBI both have a significant effect on the surface temperature of Jimma city and its surrounding. From the magnitude of the t-statistics, the expansion of settlement land had more impact on the LST confirmed by standardized coefficients.

The model also tells that with one unit increase in the vegetation, the temperature would decrease by 0.078, 0.048, and 0.022 units for the years 1987, 2003, and 2019 respectively; similarly, with one unit increase in the settlement land, there would be an increase of 0.612, 0.572 and 0.759 units in the LST for the year 1987, 2003 and 2019 respectively.

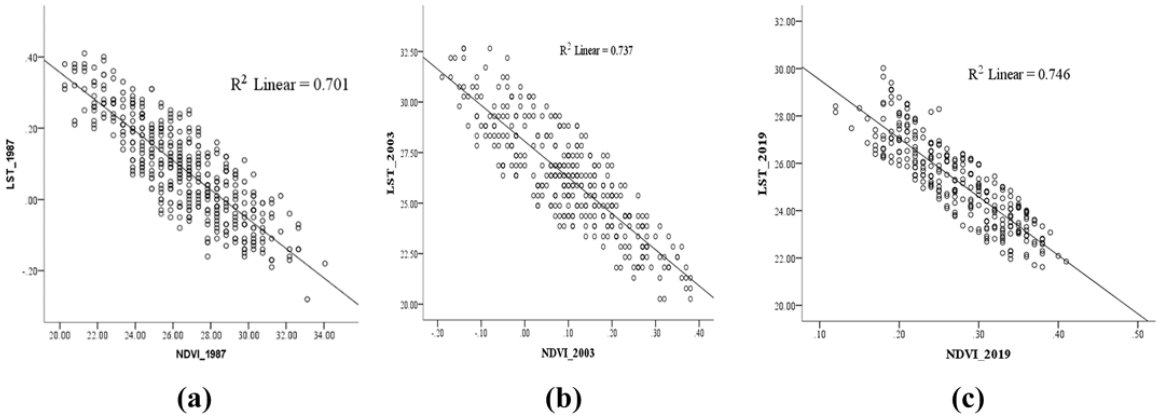

Figure 17: linear correlation between LST in response to NDVI in the year (a) 1987, (b) 2003, and (c) 2019.

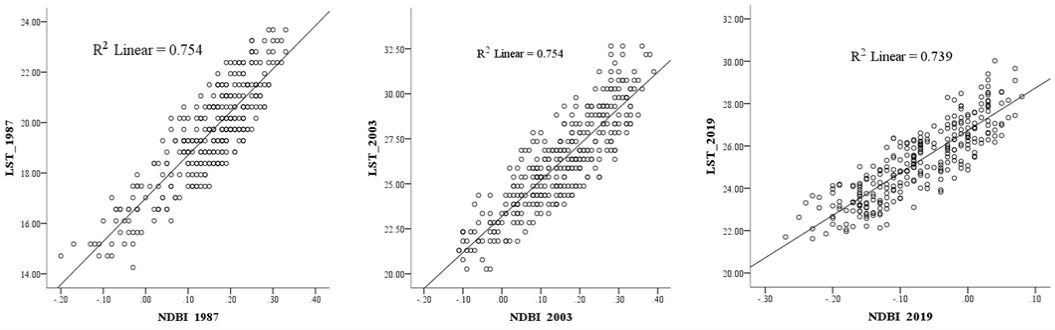

(a) **(b)** **(c)**

Figure 18: linear correlation between LST in response to NDBI in the year (a) 1987, (b) 2003, and (c) 2019.

The relationship between NDVI and NBDI has also been developed during the study. NDVI has shown a strong negative correlation with NDBI in each year i.e. $R^2 = 0.739$ in 1987 0.860 in 2003 and 0.801 in 2019. The linear correlation of NDVI vs. NDBI is displaying in the scatter plot (Figure. 18a-c).

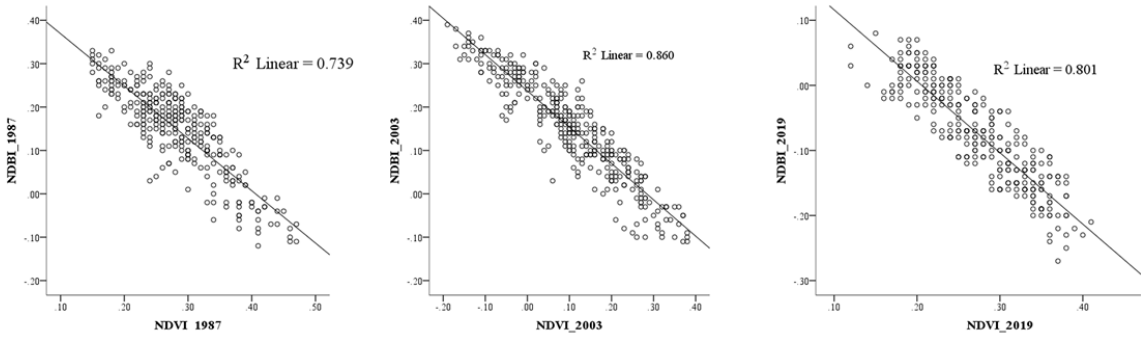

(a) **(b)** **(c)**

Figure 19: linear correlation between NDBI in response to NDVI in the year (a) 1987, (b) 2003, and (c) 2019.

4.2. Discussion

4.2.1. LULC change of the study area

LULC changes have become a major problem and a significant driving environmental change. According to FAO/UNEP (1999), LULC changes have become major problems and it is a significant driving force of environmental changes. The study conducted by Houghton (1994), indicated that human population growth, economic development, technology, and environmental changes are the major factors responsible for LULC variability. Alemayehu (2008) also showed evidence for climate change including the occurrence of drought, rising temperature, flood, reduced annual rainfall, and rising sea levels as a result of LULC changes. The major important LULC changes in the study area were land clearing for settlement and the development of infrastructure, forest to an industrial area, cropland, and mining. The study conducted by Brink *et al.,* (2014) revealed that human activities seriously affect the LULC pattern. Jianga & Tiana (2010) also discovered that urban expansion contributes to the dramatic change of LULC. The present study revealed that there were LULC changes in the study area during the study period. In 1987, the settlement area was 1096.87ha, but it reached 3057.09ha in 2019. Similarly, agricultural land was increased from 13597.6ha in 1987 to 15546.44ha in 2019. This is one of the evidence for the increasing needs of land for settlement and the removal of vegetation for agriculture. On the other hand, forest cover was decreased from 5087.52ha in 1987 to 3858.23hain 2019. Therefore, forest cover degradation/depletion was interrupted as the main cause for the loss of the ecosystem and warming of the surrounding environment. The extent of shrubland, wetland, and waterbody was also decreased from 3714.69ha, 1389.65ha, and 28.8ha in 1987 to 1624.88ha, 828.49ha, and 0ha in 2019, respectively. In general, the classified satellite images indicate that there was a change in LULC.

4.2.2. Normalized difference vegetation index

The magnitude of the NDVI is directly related to the photosynthetically active radiation and it is used to determine LST. According to Mihai (2012) and Weng (2004), NDVI is an acceptable indicator of LST and dryness. Therefore, it is used to analyze the urban environment and LST since it indicates the level of dryness and warmness of the area. The result of this study was confirmed that agricultural land and settlement areas had low NDVI

values while vegetated areas like shrubland and forest cover had high NDVI values. The correlation coefficient of NDVI and LST in 1987 was R^2 =0.701, therefore, 70.1% of LST distribution was influenced by NDVI. However, in 2017 the coefficient was R^2 = 0.746 and 74.4% of the change and distribution of LST in the study area was controlled through NDVI (vegetated areas). The present study results were also highly significant at $P < 0.01$. Because of this relationship between LST and NDVI. In line with this, the present study revealed that NDVI has strongly negatively correlated with LST. Land surface temperature and NDVI have direct relationships in different LULC categories. The water body has low NDVI and LST values.

4.2.3. LST relationships to NDBI and NDVI

It is a very interesting fact that LST distribution is very closely related to the distribution of NDVI and NDBI. Generally, LST is negatively related to NDVI and positively related to NDBI. But, this relationship may be varied from LULC type to LULC type. According to Jianga & Tiana (2010), LULC change strongly affects LST depending on the type of change. This study indicated that NDBI and NDVI in the study area vary with LULC types. It can be seen that the NDBI has a direct positive relationship with LST, while NDVI has a negative relationship with LST, as in the case of other studies like Ibrahim (2017) and Weng (2001). The densities of built-up surface and vegetation cover are important determinants of LST in urban areas, as the higher density of built-up surface raises the LST (Pramanik & Punia, 2019), while a high density of vegetation cover significantly reduces the LST (Mwangi PW, 2018).

The result of this study revealed that there was a strong negative correlation (B = -0.078) between LST and NDVI of the year 1987 and was highly statistically significant (ρ = 0.000). NDVI of the year 2003 shows a negative correlation (B = -0.048) with LST and is statistically significant (ρ= 0.000). There was also a strong negative correlation (B= -0.022) between LST and NDVI of the year 2019 and statistically significant (ρ= 0.000). In agreement with the finding of this research, (Abebe, 2018; Balew, 2018; Haylemariyam, 2018 & Asfaw, 2017) confirmed that there was a negative correlation between NDVI and LST values. LST increases with the expansion of non-vegetated areas. Agricultural land and settlement have

the lowest LST value whereas Forest land, shrubland, wetland, and waterbody class has the highest LST. The mean LST of agricultural land was 19.59˚C in 1987, 26.85˚C in 2003, and 25.82˚C in 2019. The mean temperature of shrubland was 19.15˚C in 1987, 25.14˚C in 2003, and 24.60˚C in 2019. The mean LST of the wetland was 17.50˚C in 1987, 24.68˚C in 2003, and 25.04˚C in 2019. The lowest rate of increase in LST was found under forest cover which was 17.29˚C in 1987, 22.11˚C in 2003, and 23.57˚C in 2019.

Spatial and temporal distribution of LST during 1987 and 2019 revealed that during the study period drastic changes had taken place in the area. In 1987, the distribution of LST was 12.36˚C minimum and 27.51˚C maximum, whereas in 2017 the minimum and maximum Values of LST ranges from 20.11˚C –33.68˚C, respectively.

CHAPTER FIVE

5. CONCLUSION AND RECOMMENDATIONS

5.1. Conclusion

The results of this study revealed that there was a shift in LULC during the course of the study period. The proportion of land used for settlement and agricultural purposes has been steadily rising. Waterbody, shrubland, wetland, and forest cover, on the other hand, have been declining. As a result, there were more open spaces and deforestation, resulting in a rise in LST. The lowest LST was found in areas with forest land, waterbody, wetland, and shrubland, while the greatest LST was found in areas with settlement land and agricultural land. The developed correlation of LST with NDBI and NDVI has shown $R^2 = 0.691$ in 1987, 0.774 in 2003, & 0.784 in 2019. Strong negative correlation resulted between NDVI & NDBI i.e. $R^2 = 0.739$ in 1987, 0.860 in 2003, & 0.801 in 2019, respectively. LST and NDBI have a significant positive correlation, implying that as settlement land and open land increase, so does land surface temperature. The significant negative relationship between NDVI and LST suggests that healthy green vegetation reduces surface temperature. Thus, future LST study may be collected at multiple geographical resolutions and during different seasons of the year to analyze the LST, with additional parameters like soil moisture, water bodies, and population density being utilized to determine their influence on LST. Accelerating afforestation and reforestation initiatives, as well as maintaining naturally regenerated trees, should be prioritized.

5.2. Recommendations

The focus of this study was to assess the effect of LULC change on land surface temperature in Jimma city and its surrounding between 1987 and 2019 by using space-borne multi-spectral Landsat imagery. This study revealed that LULC transformation was one of the major factors that contributed to the increasing of LST from time to time and place to place. Thus, the following feasible suggestions are forwarded based on the findings and the conclusions are drawn.

1) LULC change (specifically the reduction of green vegetation) was a serious environmental problem and its results in a rise in land surface temperature. Therefore, the governmental and non-governmental bodies should give high attention to reduce deforestation and developing strategies to decrease deforestation rates as a promotion of sustainable forest management.
2) Conservation activities have to be taken on both rural and urban green areas of the study area and recommended to plant trees and delineate green areas, especially at high-density settlement and bare land areas.
3) The study can be used for further research in the area of land-use and land-cover and its impact.
4) The use of a liner regration model in a GIS context, which integrated climatic, topography, and remotely sensed data, was found to be extremely useful in assessing past and present forest cover and land surface temperature status, from which suitable future planning could be formed. To plan appropriate forest management schemes and develop required management safeguards, knowledge of cause-effect connections between forest cover and land surface temperature models should be crucial.

REFERENCES

Aadil, M., Rafiq, A., Aadil, H. & Pervez, A., 2014. Changes in land-use/land-cover dynamics using geospatial techniques: A case study of Vishav drainage basin. *J. Geogr. Reg. Plan.,* 7, pp. 69–77.

Abate, S., 2011. Evaluating the land use and land cover dynamics in Borena Woreda of South Wollo highlands, Ethiopia. *J. Sustain. Dev. Afr.,* 13, pp. 87–105.

Abbas, I., Muazu, M. & Ukoje, J., 2010. Mapping land use-land cover and change detection in Kafur local government, Katsina, Nigeria (1995-2008) using remote sensing and GIS. *J. Environ. Earth Sci.,* 2, pp. 6-12.

Abebe, M. S., Derebew, K. T. & Gemeda, D. O., 2019. Exploiting temporal-spatial patterns of informal settlements using GIS and remote sensing technique: a case study of Jimma city, Southwestern Ethiopia. *Environ Syst Res,* 8(6).

Abrha, C., Feyisa, G. L. & Feyssa, D. H., 2015 . Analysis of land use/cover dynamics in Jimma city, Southwest Ethiopia: an application of satellite remote sensing. *Ethiop.J.Appl.Sci. Technol.,* 6(2), pp. 24-34.

Agarwal, C., Green, G.M., Grove, J.M., Evans, T.P., & Schweik, C.M., 2002. A Review and Assessment of Land-Use Change Models: Dynamics of Space, Time, and Human Choice. General Technical Report NE-297. Newtown Square, Pennsylvania: U.S. Department of Agriculture, Forest Service, Northeastern Research Station.

Ahl, D.E., Gower, S.T., Burrows, S.N., Shabanov, N.V., Myneni, R.B., & Knyazikhin, Y., 2006. Monitoring spring canopy phenology of a deciduous broadleaf forest using MODI. *Remote Sens. Environ.,* 104, pp. 88–95.

Alemu, B., Garedew, E., Eshetu, Z. & Kassa, H., 2015. Land use and land cover changes and associated driving forces in Northwestern low lands of Ethiopia. *International Research Journal of Agricultural Science and Soil Science,* 5(1), pp. 28–44.

Ali-Toudert, F. & Mayer, H., 2007. Effects of asymmetry, galleries, overhanging facades and vegetation on thermal comfort in urban street canyons. *Sol. Energy,* 81, pp. 742-754.

Alqurashi, A. & Kumar, L., 2013. Investigating the Use of Remote Sensing and GIS Techniques to Detect Land Use and Land Cover Change: A Review. *Advances in Remote Sensing,* 2, pp. 193-204 .

Alshaikh, A., 2015.Vegetation cover density and land surface temperature interrelationship using satellite data, case study of Wadi Bisha, South KSA. *Advances in Remote Sensing,* 4, pp. 248-262.

Amiri, R., Weng, Q., Alimohammadi, A. & Alavipanah, S., 2009. Spatial–temporal dynamics of land surface temperature in relation to fractional vegetation cover and land use/cover in the Tabriz urban area, Iran. *Remote Sens. Environ.,* 113, pp. 2606-2617.

Ariti, A. T., Vliet, J. V. & Verburg, P. H., 2015. Land-use and land-cover changes in the Central Rift Valley of Ethiopia: Assessment of perception and adaptation of stakeholders. *AppliedGeography,* 65, pp. 28–37.

Arvor, D., Dubreuil, V., Simões, M. & Bégué, A., 2014. Mapping and spatial analysis of the soybean agricultural frontier in Mato Grosso, Brazil, using remote sensing data. *GeoJournal,* 78, pp. 833–850.

Asner, P. G., Rudel, .. K. T. & Aid, M. T., 2009. 2009. A Contemporary Assessment of Change in Humid Tropical Forests. *Conservation Biology,* 3(6), pp. 1386–1395.

Balew, A., 2018. Impacts of Land-Use and Land-Cover Changes on Land Surface Temperature Distribution in Bahir Dar Town and Its Surroundings Using Remote Sensing. Msc thesis.

Barsi, J.A., Schott, J.R., Hook, S.J., Raqueno, N.G., Markham, B.L., & Radocinski, R.G., 2014. Landsat-8 thermal infrared sensor (TIRS) vicarious radiometric calibration. *Remote Sens.,* 6, pp. 11607–11626.

Becker, F. & Li, Z. L., 1990. Towards a local split window method over land surfaces. *Remote Sensing,* 11(3), p. 369–393.

Chala, T. E., 2010. An Assessment of Forest Resource Conservation and Development Strategy in the Case of Ameya Woreda South West Shewa Zone, Oromia Regional State. *reaserch thesis, Addis Ababa University* .

Chen, D., Wang, X., Khoo, Y.B., Thatcher, M., Lin, B.B., Ren, Z., Barnett, G., 2013. Assessment of urban heat island and mitigation by urban green coverage. *In Mitigating climate change (Springer Berlin Heidelberg),* pp. 247-257.

Claus, R. & Mushtaq, H., 2011. Toronto's Urban Heat Island: Exploring the Relationship between Land Use and Surface Temperature. *Remote Sens.,* 3, pp. 1251–1265.

Congalton, R., 1991. A review of assessing the accuracy of classifications of remotely sensed data. *Remote Sensing of Environment,* 37(1), pp. 35-46.

Coskun, H. G., Alganci, U. &Usta,G.,2008.Analysis of Land Use Change and Urbanization in the Kucukcekmece Water Basin (Istanbul, Turkey) with Temporal Satellite Data using Remote Sensing and GIS. *Sensors,* 8, pp. 7213-7223.

CSA, 2013. Population Projection of Ethiopia for All Regions At Wereda Level from 2014 – 2017, Addis Ababa : Federal Democratic Republic of Ethiopia Central Statistical Agency.

David, W.P. & Corin, G.P., 2001. The Value of Forest Ecosystems. *A Report to The Secretariat ,* Issue Convention on Biological Diversity .

Demel, T., 2010. Forest resources and challenges of sustainable forest management and conservation in Ethiopia.In: F.Bongers, & T.Tennigkeit, (eds). Degraded forests in Eastern Africa. Management and Restoration. Earthscan Publications.

Deribew, K. T. & Dalacho, D. W., 2019. Land use and forest cover dynamics in the North-eastern Addis Ababa, central highlands of Ethiopia. *Environ Syst Res ,* 8(8), pp. 1-18.

Donato, S., Sebastiano, C. & Sebastiano, S. F. G., 2016. Anthropogenic Influences in Land Use/Land Cover Changes in Mediterranean Forest Landscapes in Sicily. Land 5.

Dube, E. E., 2013 . Urban planning and land management challenges in emerging towns of Ethiopia: the case of Arba Minch. *Journal of Urban and Environmental Engineering ,* 7(2), pp. 340-348.

EARO, 2008. Draft strategy and action plan for integrated forest development in Ethiopia.. *Forestry Research Center, Addis Ababa,* pp. 11.

Elijah, K. M., 2007. Deforestation and Afforestation, A world perspective With Three Case Studies in Brazil, Nigeria, and Japan Paper For NRES 523 International Resource Management..

FAO, 2000. State of world's forests 2000. Rome.

FAO, 2010. Global Forest Resources Assessment 2010. Main report. *Food and Agriculture Organization of the United Nations:Rome, Italy.*

FAO, 2012. State of the World‟s forests. Food and Agriculture Organization of the United Nations, Rome, Italy. pp. 6-10.

FAO, 2015. GlobalForest Resources Assessments. *Food and Agriculture Organization of the United Nations: Rome, Italy.*

Farooq, A., Qurat-ul-ain, F., Hir, J.B., Kashi, S., Sajid, R.A. & Shafeeq-Ur, R., 2013. *Glob J Hum Soc Sci ,* 13, pp. 21–42.

Fei, Z., Tashpolat, T., Hsiangte, K., Verner, C.J., Matthew, M., Mei, Z.& Juan, W., 2016. Dynamics of land surface temperature (LST) in response to land use and land cover (LULC) changes in the Weigan and Kuqa river oasis, Xinjiang, China. *Arab J Geosci. ,* 9(499).

Fenglei, F., Yunpeng, W., Maohui, Q. & Zhishi, W., 2009. Evaluating the Temporal and Spatial Urban Expansion Patterns of Guangzhou from 1979 to 2003 by Remote Sensing and GIS Methods. *Int. J. Geogr. Inf. Sci.,* 23, pp. 1371–1388.

FWCDA, 1982. Forestry for Community Development. Addis Ababa, Ethiopia.

Gao, J., 2009. Digital Analysis of Remotely Sensed Imagery. McGraw-Hill.

Gao, J. & Liu, Y., 2012. "De (re)forestation and climate warming in subarctic China,". *Appl. Geogr,* 32, pp. 281-290.

Garai, D. & Narayana, A., 2018. Land use/land cover changes in the mining area of Godavari coal fields of southern India. *EJRS,* 21, pp. 375-381.

Gebrekidan, W., 2016. Modeling land surface temperature from satellite data, the case of Addis Ababa. ES RI, Eastern Africa Education GIS conference. Held at Africa hall, United Nations conference center from23-24 sept. 2016, Addis Ababa.

Gluch, R., Quattrochi, D. & Luvall, J., 2006. A multiscale approach to urban thermal analysis. *Remote Sens. Environ.,*104, pp. 123–132.

Grover, A. & Singh, R., 2015. Analysis of urban heat island (UHI) in relation to normalized difference vegetation index (NDVI): A comparative study of Delhi and Mumbai.. *Environ.,* 2, pp. 125-138.

Harvith, J., 1968. Addis Ababa Eucalyptus Forest. *Journal of Ethiopian Study,* 6, pp. 24-37.

Haylemariyam, M. B., 2018. Detection of Land Surface Temperature in Relation to Land Use Land Cover Change: Dire Dawa City, Ethiopia. *Journal of Remote Sensing & GIS,* 7(3).

Huang, S. & Siegert, F., 2006. Land cover classification optimized to detect areas at risk of desertification in North China based on SPOT VEGETATION imagery. *J. Arid Environ.,* 67, pp. 308–327.

Hu, Y. & Jia, G., 2010. Influence of land use change on urban heat island derived from multi-sensor data.,. *Int. J. Climato.,* 30, pp. 1382-1395 .

Igun, E. & Williams, M., 2018. Impact of urban land cover change on land surface temperature. *Global J. Environ. Sci. Manage.,* 4(1), pp. 47-58.

IPCC, 2014. *Climate Change 2014 Synthesis Report,* Switzerland : World Meteorological Organization .

Jianga, J. & Tiana, G., 2010. Analysis of the impact of Land use/Land cover change on Land Surface Temperature with Remote Sensing. *Procedia Environ. Sci.,* 2, pp. 571-575.

John, W. & David, H., 1999. *(1999), Measuring Vegetation (NDVI & EVI), Earth Observatory.* USA: NASA.

Kayet, N., Pathak, K., Chakrabarty, A. & Sahoo, S., 2016. Spatial impact of land use/land cover change on surface temperature distribution in Saranda Forest, Jharkhand. *Modeling Earth Systems and Environment,* 2(3) , pp. 1–10.

Kerr, Y., Lagouarde, J., Nerry, F. & Ottle, C., 2004. Land surface retrieval techniques and applications: case of AVHRR, in: Quatrocci, D.A., Luvall, J. C. Thermal remote sensing in land surface processes. CRC press, Florida, USA. pp. 33–109.

Khin, M., D.Y., S., Park, J. & C.C., C., 2012. Land surface temperature changes by LU changes of Inlay Lake area, Myanmar. Department of Spatial Information Engineering, Pukyong National University, South Korea.

Kumar, R. & Singh, S., 2016. Case Study for Change Detection Analysis and Land Surface Temperature Retrieval in Uttrakhand Region and their correlation. *Imperial Journal of Interdisciplinary Research,* 2(9).

Lilly R., A. & Devadas, M., 2009. Analysis of land surface temperature and land use/land cover types using remote sensing imagery-a case in Chennai city, India. *In The seventh International Conference on Urban Climate.*

Liu, L. & Zhang, Y., 2011. Urban heat island analysis using the Landsat TM data and ASTER data: A case study in Hong Kong. *Remote Sens.,* 3, pp. 1535–1552.

Mahmood, R. R., A., Pielke, SR.R., kenneth, G., Hubbard, niyogi, D., Gordon, B.; Peter, L., Richard, Mc., Clive, Mc., Andres, E., Samuel, G.& Budong, Q., 2010. Impacts of land use/land cover change on climate and future research priorities. *Bulletin of the American Meteorological Society,* 91, pp. 37-46.

Maimatiyiming, M., Ghulam, A., Tiyip, T., Pla, F., Latorre-Carmona, P., Sawut, M., Halik, U.& Caetano, M., 2014. Effects of spatial pattern of green space on land surface temperature: implications for sustainable urban planning and climate change adaptation. *ISPRS J Photogramm Remote Sens.,* 89, pp. 59–66.

Malik, M., Shukla, J. & Mishra, S., 2019. Relationship of LST, NDBI and NDVI using Landsat-8 data in Kandaihimmat Watershed, Hoshangabad, India. *Indian Journal of Geo Marine Sciences,* 48(01), pp. 25-31 .

Mallick, Y. & Kerle, C., 2006. Satellite-based Analysis of the Role of Land Use! Land Cover and Vegetation Density on Surface Temperature Regime of Delhi, India. *J Indian Soc Remote Sens,* 37, pp. 201-214.

Manea, D., Manea, E. & Robescu, D., 2013. Study on greenhousegas emissions from wastewater treatment plants. *Environ. Eng. Manag. J.,* 12, pp. 59-63.

Mather, A. S., 2014. Global Trends in Forest Resources. *Geographical Association,* 72(1), pp. 1-15.

Matthews, E., 1982. Global Vegetation and Land use: New High Resolution Databases for Climatic Study. *Journal of Climate and Applied Meteorology,* 22, pp. 474-487.

MEFCC, 2015. Ethiopia Forest Sector Review. Focus on commercial forestry and industrialization. UNIQUE forestry and land use / CONSCIENTIA, Addis Ababa, Ethiopia.

MEFCC, 2016. Ethiopia's Forest Reference Level Submission To The UNFCCC. Addis Abeba, Ethiopia.

Meijun, J., Junming, L., Caili, W. & Ruilan, S., 2015. A Practical Split-Window Algorithm for Retrieving Land Surface Temperature from Landsat-8 Data and a Case Study of an Urban Area in China. *Remote Sens.,* 7, pp. 4371–4390.

Mohan, M. & Kandya, A., 2015. Impact of urbanization and land-use/landcover change on diurnal temperature range: a case study of tropical urban airshed of India using remote sensing data.. *Sci Total Env.,* 506, pp. 453–465.

Mosammam, H.M., Nia, J.T., Khani, H., Teymouri, A.& Kazemi, M., 2017. Monitoring land use change and measuring urban sprawl based on its spatial forms. The case of Qom city. *Egypt J Rem Sens Space Sci.,* 20, pp. 103–116.

Musa, T., Xu, W., W., Hou., Terence, D. M.& Sen, C., 2018. Effect of Deforestation on land surface Temprature: A Case of Freetown and Botown in Sierra Leone. pp. 5232-5235.

NASA, 2000. Landsat 7 Science Data Users Handbook.

Nuruzzaman, M., 2015. Urban Heat Island: Causes, Effects and Mitigation Measures-A Review. *International Journal of Environmental Monitoring and Analysis,* 3(2), pp. 67.

Onishi, A., Cao, X., Ito, T., Shi, F.& Imura, H., 2010. Evaluating the potential for urban heat-island mitigation by greening parking lots. *Urban For Urban Greening,* 9, pp. 323-332.

Orimoloye, I., Mazinyo, S., Nel, W. & Kalumba, A., 2018. Spatiotemporal monitoring of land surface temperature and estimated radiation using remote sensing: human health implications for East London, South Africa. *Environ. Earth Sci.,* 77(77), pp. doi:10.1007/s12665-018-7252-6.

Paramasivam, C., 2016. Remote Sensing and spectral studies of magnesite mining area, Salem, India. For the award of the Degree of Doctor of Philosophy in Geology thesis submitted to Periyar University, Salem, India.

Peter, M., 1994. Beyond Global Warming: Ecology and Global Change. *Ecol. Soc. Am.,* 75, pp. 1861–1876.

Polydoros, A., Mavrakou, T. & Cartalis, C., 2018. Quantifying the Trends in Land Surface Temperature and Surface Urban Heat Island Intensity in Mediterranean Cities in View of Smart Urbanization. *Urban Science,* 2(1), pp. 16.

Pongratz, J., Reick, C. H., Raddatz, T. & Claussen, M., 2010. Biogeophysical versus biogeochemical climate response to historical anthropogenic land cover change Geophys. *Res. Lett.,* 37 (16), pp. 2–9.

Qijiao, X. & Zhixiang, Z., 2015. Impact of urbanization on urban heat island effect based on TM imagery in Wuhan, China. *Environ. Eng. Manag. J.,* 14, pp. 647–655.

Rajeshwari, A. & Mani, N. D., 2014. Estimation of land surface temperature of Dindigul Woreda using Landsat 8 data. *International Journal of Research in Engineering and Technology,* 3(5), pp. 122–126.

Rao, K. S. & Pand, R., 2001. land use dynamics and landscape change pattern in a typical microwatershed in the mid elevation zone of central Hemalaya, India. *Agri. Ecosyst. Environ.,* 86, pp. 113-124.

Raynolds, M., Comiso, J., Walker, D. & Verbyla, D., 2008. Relationship between satellite-derived land surface temperatures, arctic vegetation types, and NDVI. *Remote Sens. Environ.,* 112, pp. 1884-1894.

Richards, J. & Jia, X., 2006. *Remote Sensing Digital Image Analysis: An introduction.* 4th ed. Germany: Springer-Verlag Berlin Heidelberg 2006.

Roberts, D.A., Dennison, P.E., Roth, K.L., Dudley, K.& Hulley, G., 2015. Relationships between dominant plant species, fractional cover and Land Surface Temperature in a Mediterranean ecosystem. *Remote Sensing of Environment,* 167, pp. 152-167, (https://doi.org/10.1016/j.rse.2015.01.026).

Rotem-Mindali, O., Michael, Y., Helman, D. & Lensky, I. M., 2015. The role of local land-use on the urban heat island effect of Tel Aviv as assessed from satellite remote sensing. *Appl. Geogr.,* 56, pp. 145-153.

Russell, G., Congalton & Kass, G., 2019. *Assessing the Accuracy of Remotely Sensed Data: Principles and Practices.*3rd ed. Inc., Boca Raton, London, New York, Washington DC: CRC press.

Sahana, M., Ahmed, R. & Sajjad, H., 2016. Analyzing land surface temperature distribution in response to land use/land cover change using split-window algorithm and spectral radiance model in Sundarban Biosphere Reserve, India. *Modeling Earth Systems and Environment,* 2, pp. 81.

Sahoo, S., 2013. Monitoring urban Land use land cover change by multi-temporal remote sensing information in Howrah City, India. *Int. Res. J. Earth Sci.,* 1(5), pp. 1–6.

Saleh, S., 2010. Impact of urban expansion on surface temperature in Baghdad, Iraq using remote sensing and GIS techniques. *Journal of AlNahrain University-Science,* 13, pp. 48-59.

Small, C., 2004. Global population distribution and urban land use in geophysical parameter space. *Earth Interact.,* 8, pp. 1–18.

Sobrino, J.A., Rosa, O., Guillen, S., Juan, C.J., Belen.F., Victoria.H., Cristian, M., Yves, J., Juan, C., Mireia, R., Antonio, G.J., Eduardo, D.M., Remo, B.& Marc, p., 2012. Evaluation of the surface UHI effect in the city of Madrid by thermal R. *International journal of remote sensing,* 34, pp. 910.

Streutker, D. R., 2003. Satellite-measured growth of the urban heat island of Houston, Texas. *Remote Sensing of Environment,* 85(3), pp. 282–289.

Sun, Q., Wu, Z. & Tan, J., 2012. The relationship between land surface temperature and land use/land cover in Guangzhou, China. *Environ. Earth Sci.,* 65, pp. 1687–1694.

Tang, Z., Shi, C. & Bi, K., 2014. Impacts of land cover change and socioeconomic development on ecosystem service values. *Environ. Eng. Manag. J.,* 13, pp. 2697–270.

Temesgen, G., Amare, B. & Abraham, M., 2014. Evaluations of Land Use/Land Cover Changes and Land Degradation in Dera District, Ethiopia: GIS and Remote Sensing Based Analysis. *Int. J. Sci. Res. Environ. Sci.,* 2, pp. 199–208.

UN, 2014. World Urbanization Prospects: The 2014 Revision, Highlights (No. ST/ESA/SER.A/352). United Nations, Department of Economic and Social Affairs, Population Division, New York.

UNEP, 2011. Billion Tree campaign website.

UN-HABITAT, 2010. State of the World's Cities 2010/2011: Prosperity of Cities. Earthscan, UK, United Nations Human Settlements Programme.

UN-HABITAT, 2913. State of the World's Cities 2012/2013: Prosperity of Cities. Routledge Taylor & Francis Group, United Nations Human Settlements Programme, New York..

USGS, 2019. *Landsat 8 (L8) Data Users Handbook..* 5 ed. s.l.:Department of the Interior U.S. Geological Survey.

Veldkamp, A. & Lambin, E., 2001. Predicting land-use change. *Agric. Ecosyst. Environ.,* Volume 85, pp. 1-6.

Voogt, J., 2000. *How researchers measure UHI.* 2nd ed. Canada: Glossary of Meteorology.

Wang, F., Qin, Z., Song, C., Tu, L., Karnieli, A.& Zhao, S., 2015. An improved mono-window algorithm for land surface temperature retrieval from Landsat 8 thermal infrared sensor data. *Remote Sens.,* 7, pp. 4268–4289.

WBISPP, 2004. A strategic plan for the sustainable development, conservation And management of the woody biomass resources. Final report. *Federal Democratic Republic of Ethiopia, Ministry of Agriculture,* pp. 60.

Weng, Q. & Lu, D., 2008. A sub-pixel analysis of urbanization effect on land surface temperature and its interplay with impervious surface and vegetation coverage in Indianapolis, United States. *Int. J. Appl. Earth Obs. Geoinf.,* 10, pp. 68-83.

Weng, Q., Lu, D. & Schubring, J., 2004. Estimation of land surface temperature–vegetation abundance relationship for urban heat island studies. *Remote Sens. Environ.,* 89, pp. 467-483.

Western Oromia region Meteorology Center, 2019. *Jimma Town Rain fall and tempreture distribution.,* Jimma: unpublished data.

William, B. & Turner, B., 1992. Human Population Growth and Global Land-Use/Cover Change. *Annu. Rev. Ecol.,* 23, pp. 39-61.

Williams, M., 2003. Deforesting the Earth: from Prehistory to Global Crisis.. *UniversityofChicagoPress, Chicago,* IL, pp. 689 .

Wilson, E.H., Hurd, J.D., Civco, D.L., Prislof, M.P.& Arnold, C., 2003. Development of a geospatial model to quantify, describe and map urban growth. *Remote Sens. Environ.,* 86, pp. 275-285.

Wim, H., Ambro, S. M. & Ben, G. H. G., 2004. *Principles of Remote Sensing: An introductory textbook.* 3rd ed. Netherlands: The International Institute for Geo-Information Science and Earth Observation (ITC), Hengelosestraat 99.

Wogderes, A., 2014. Detecting land use/land cover change using remote sensing & GIS techniques and analysis of its causes, consequences and trends.Thesis(M.Sc.).Ofla woreda,tigrayregion,Ethiopia. Addis Ababa University.

Woodcock, C., Macomber, S. & Kumar, L., 2002. Vegetation Mapping and Monitoring. In: Skidmore, A.K. Environmental Modelling with GIS and Remote Sensing. Taylor and Francis, London, UK.

Xiong, Y., Huang, S., Chen, F., Ye, H., Wang, C.& Zhu, C., 2012. The impacts of rapid urbanization on the thermal environment: a remote sensing study of Guangzhou, South China. *Remote Sens.,* 4, pp. 2033–2056.

Yadvinder, M. J., Timmons, R., Richard, A.B., Timothy, J.K., Wenhong, L.& Carlos, A.N., 2008. Climate Change, Deforestation, and the Fate of the Amazon. *Science.,* 319, pp. 169-172.

Yue, W., Xu, J., Tan, W. & Xu, L., 2007. The relationship between land surface temperature and NDVI with remote sensing: application to Shanghai Landsat 7 ETM+ dat. *Int. J. Remote Sens.,* 28, pp. 3205–3226.

Zeleke, G. & Hurni, H., 2001. Implication of land use and land cover dynamics for mountain resource degradation in the northwestern Ethiopia highlands.. *Mt Res Dev,* 21, pp. 184–191.

Zengin, H., Degermenci, A. & Bettinger, P., 2018. Analysis of tempAnalysis of temporal changes in land cover and landscape metrics of a managed forest in the West Black Sea region of Northern Turkey: 1970–2010. *J. For. Res.,* 29, pp. 139-150.

Zha, Y., Gao, J. & S., N., 2003. Use of normalized difference built-up index in automatically mapping urban areas from TM imagery. *International Journal of Remote Sensing,* 24(3), pp. 583-594.

Zheng, B., Myint, S. & Fan, C., 2014. Spatial configuration of anthropogenic land cover impacts on urban warming. *Landsc. Urban Plan.,* 130, pp. 104–111.

Zhibin, R., Haifeng, Z., Xingyuan, H., Dan, Z.& Xingyang, Y., 2015. Estimation of the relationship between urban vegetation configuration and land surface temperature with remote sensing. *J. Indian Soc. Remote Sens.,* 43, pp. 89-100 .

Appendixes

Appendix I: Image Interpretation and Classification Ground Control Points

		1987		2003		2019		
ID	Zone	East	North	East	North	East	North	LULC
1	37	257062.5	854054.5	258667.8	855182.1	267345.6	846973.4	Forest
2	37	256666.7	857638.9	258717.7	854818.0	267538.3	845993.8	Forest
3	37	258973.1	854631.6	259005.5	854693.3	266728.4	847369.4	Forest
4	37	256632.7	853859.5	259118.9	854987.5	265369.5	849761.7	Forest
5	37	255638.3	852955.5	259908.7	855694.2	265985.8	849848.8	Forest
6	37	253083.0	852959.3	259098.9	854816.6	264237.3	851978.1	Forest
7	37	253553.1	856459.4	256932.8	854109.9	264005.9	850949.6	Forest
8	37	254014.4	854428.3	257237.8	853842.6	263008.9	853049.1	Forest
9	37	254930.3	850870.5	254417.4	850099.1	260439.7	854542.0	Forest
10	37	254617.3	850210.8	252678.4	853464.2	261647.2	854156.0	Forest
11	37	251585.4	849903.9	254228.8	850547.1	259576.4	854042.8	Forest
12	37	250115.3	850393.8	254016.4	850305.7	259731.4	854130.6	Forest
13	37	250941.2	851003.2	254192.8	850611.4	258803.1	854732.9	Forest
14	37	252592.7	850538.8	258160.1	850726.0	257185.0	853815.3	Forest
15	37	261373.1	853173.6	258294.5	851053.1	256632.6	853479.7	Forest
16	37	260497.7	856673.8	258555.8	851293.2	256558.0	854003.1	Forest
17	37	259786.1	854204.8	255291.1	848782.9	252888.9	852371.7	Forest
18	37	260088.9	854303.4	251548.8	849905.4	256567.7	852668.9	Forest
19	37	260298.2	853422.4	265112.1	849560.8	256766.1	852191.9	Forest
20	37	263749.0	861086.4	265282.7	849371.4	259332.7	851695.6	Forest
21	37	264328.0	858019.6	264167.2	851473.6	258763.0	851208.6	Forest
22	37	263977.6	851498.5	265667.3	849343.1	260715.7	851303.0	Forest
23	37	265447.2	849800.4	264170.7	850875.1	258103.8	850711.2	Forest
24	37	265931.6	849600.3	265809.7	848817.2	258579.7	850117.6	Forest
25	37	265586.5	848855.0	265895.8	848519.7	258144.0	850172.2	Forest
26	37	265932.2	848236.8	265291.3	849325.1	259281.9	844753.9	Forest
27	37	265595.1	848244.2	265864.9	848732.8	257304.7	845970.2	Forest
28	37	265880.0	847830.6	265975.1	848032.7	257723.7	845891.5	Forest
29	37	266452.0	847835.1	265650.8	847866.8	257132.0	845650.8	Forest
30	37	267478.1	847342.9	265971.8	847698.8	257777.0	843780.5	Forest
31	37	267073.6	846859.4	266563.6	847635.4	258352.4	843844.9	Forest
32	37	267875.3	846268.5	267486.1	847202.7	259314.0	844114.7	Forest
33	37	261539.4	849405.7	267133.2	846902.3	259168.8	845957.4	Forest
34	37	260089.9	849372.2	267041.3	847204.1	257598.3	846843.4	Forest
35	37	264622.0	847550.7	267427.5	846298.2	265839.9	847580.4	Forest
36	37	261190.3	848893.2	260785.1	848861.5	262958.6	848531.6	Settlement
37	37	261198.1	848599.8	261198.7	848754.4	262017.6	848180.1	Settlement
38	37	261036.5	848553.4	261279.4	848598.1	261027.9	848224.9	Settlement

39	37	260785.8	849253.9	261021.2	848522.6	261205.9	848733.5	Settlement
40	37	260784.9	848204.3	261246.7	848254.3	262881.6	849899.7	Settlement
41	37	260894.8	847998.1	261235.1	848181.7	264194.5	849387.6	Settlement
42	37	260891.9	848262.0	261027.3	848186.1	263291.9	848978.2	Settlement
43	37	261074.7	848951.4	260962.1	848502.3	263212.1	849342.5	Settlement
44	37	261205.8	848306.8	260896.4	848179.5	263020.9	849280.3	Settlement
45	37	261691.7	848147.2	261259.3	848168.5	264919.2	848426.9	Settlement
46	37	262779.7	847806.1	260803.0	848602.8	264325.1	848356.3	Settlement
47	37	262575.4	848303.4	260946.8	848529.6	262946.8	846608.1	Settlement
48	37	262632.3	848560.8	260629.0	848171.7	262966.1	847596.2	Settlement
49	37	261200.9	849296.8	260481.7	848188.8	261977.1	847356.4	Settlement
50	37	261170.1	848734.0	260944.9	848100.7	260806.7	846599.8	Settlement
51	37	261097.3	849254.6	261051.7	848064.8	259589.1	847433.6	Settlement
52	37	260975.4	849052.7	261370.1	848128.6	259538.9	847981.7	Settlement
53	37	261318.0	848996.7	261604.4	848187.6	262530.2	846517.5	Settlement
54	37	261017.4	848084.8	261712.8	847972.5	262083.7	845511.1	Settlement
55	37	268379.2	849069.8	261637.8	847641.6	261527.5	845733.5	Settlement
56	37	259690.0	847562.9	261587.0	847827.0	259294.5	845483.8	Settlement
57	37	262589.0	849250.5	261885.5	848058.2	259734.3	846020.7	Settlement
58	37	263223.1	849875.9	261739.1	848163.8	264661.7	850775.7	Settlement
59	37	263333.8	848929.0	262111.2	847168.8	265573.7	851543.6	Settlement
60	37	260095.0	849998.5	262160.5	847153.9	259797.0	850550.8	Settlement
61	37	259736.8	849102.5	261207.6	849050.3	259561.1	850389.7	Settlement
62	37	260143.5	848987.0	260855.0	849051.8	259392.9	849653.6	Settlement
63	37	260132.1	849451.8	260462.8	848988.5	258747.3	849005.2	Settlement
64	37	259162.2	849283.0	260869.5	847974.6	258590.2	849149.5	Settlement
65	37	259318.5	849752.4	260959.2	847823.9	260969.3	848295.7	Settlement
66	37	260525.0	849807.1	259897.1	847604.9	260950.5	848046.8	Settlement
67	37	260263.3	849653.1	259210.3	847906.1	261295.2	847602.5	Settlement
68	37	261693.9	849248.5	259291.9	848067.0	262252.7	847518.9	Settlement
69	37	261535.3	849044.3	259935.1	849007.9	262326.1	847624.3	Settlement
70	37	260194.5	848770.1	260512.4	848502.7	262668.1	847820.7	Settlement
71	37	261474.9	849415.3	257974.0	855301.5	266969.1	846726.5	Shrubland
72	37	260087.5	849439.1	258222.8	855155.3	267131.1	846666.9	Shrubland
73	37	259590.4	850199.9	264216.8	855105.9	266099.2	847799.1	Shrubland
74	37	259634.2	848702.0	258120.2	854895.4	265278.1	848244.3	Shrubland
75	37	260077.8	847854.3	258989.7	854666.8	265089.2	847989.4	Shrubland
76	37	260972.5	846989.4	256878.4	852265.4	259645.3	851405.9	Shrubland
77	37	260466.7	849421.6	258379.6	850557.6	259661.5	851444.5	Shrubland
78	37	260078.7	849441.4	258643.8	850644.8	261635.2	846090.4	Shrubland
79	37	261376.7	849250.7	258484.4	850639.8	259632.9	851468.8	Shrubland
80	37	261498.5	849489.8	258651.1	850677.5	259077.1	845933.9	Shrubland
81	37	261551.5	849826.2	258453.8	850622.1	261421.9	852804.3	Shrubland

82	37	259593.1	850243.0	258965.5	854731.5	259636.9	851410.5	Shrubland
83	37	260061.9	848530.3	258303.7	849909.2	258700.1	851007.8	Shrubland
84	37	261234.5	850242.9	258337.3	849936.2	258637.2	851013.0	Shrubland
85	37	261200.8	850439.6	258428.4	849586.8	258389.7	851388.0	Shrubland
86	37	261166.3	849929.6	259692.7	850348.2	261424.6	852805.4	Shrubland
87	37	261046.9	849615.0	256878.4	852265.4	261403.0	852792.9	Shrubland
88	37	261283.8	849243.1	259975.0	850696.6	262199.8	853105.7	Shrubland
89	37	260808.5	849215.8	258759.3	849205.9	257528.0	850774.7	Shrubland
90	37	261512.6	849109.4	259681.6	849066.1	253658.1	849185.7	Shrubland
91	37	260129.0	849071.3	260419.4	849015.1	262250.2	853013.7	Shrubland
92	37	260002.1	848501.5	259689.5	849109.3	262260.0	853006.7	Shrubland
93	37	258524.6	848973.7	260055.1	846527.7	258404.7	849569.8	Shrubland
94	37	258325.8	849000.6	260074.1	846430.1	258385.4	849898.1	Shrubland
95	37	258410.2	848894.5	262014.6	846340.0	258261.0	849943.4	Shrubland
96	37	258556.9	850179.2	259365.1	846859.2	264790.5	848950.2	Shrubland
97	37	256846.2	848856.9	259364.8	846250.0	262199.2	853104.4	Shrubland
98	37	264372.3	845321.0	260033.9	846583.8	262533.8	853164.8	Shrubland
99	37	264249.0	845092.9	259614.0	849084.2	260699.7	843770.2	Shrubland
100	37	262118.3	847629.7	260055.1	846527.7	257597.1	844225.3	Shrubland
101	37	261751.4	847517.9	259313.5	855925.4	256507.8	846406.6	Shrubland
102	37	260045.3	848523.4	258222.8	855155.3	256302.6	845978.6	Shrubland
103	37	260065.4	849417.5	258706.0	850569.0	256466.2	845820.1	Shrubland
104	37	260473.8	849397.6	256918.0	852226.8	256559.6	847036.8	Shrubland
105	37	260533.4	849220.6	258436.7	850600.2	258309.2	847500.7	Shrubland
106	37	257574.3	848661.0	252789.9	854205.0	260189.7	844620.0	Agriculture
107	37	258610.3	848003.2	250268.4	853127.9	262905.7	844560.5	Agriculture
108	37	260374.8	846717.9	251391.4	850934.1	266127.1	846743.9	Agriculture
109	37	258902.7	848585.8	253077.3	850967.6	265031.7	847058.7	Agriculture
110	37	259174.7	845484.3	253113.1	850967.3	259069.7	849629.9	Agriculture
111	37	261497.3	849427.0	255461.2	850586.7	259077.8	849482.4	Agriculture
112	37	261895.5	845564.0	258741.5	853079.1	256429.4	847683.0	Agriculture
113	37	263559.1	844628.1	262401.8	854858.3	258875.3	849608.2	Agriculture
114	37	264516.2	845955.6	263219.8	854178.9	259221.3	849403.7	Agriculture
115	37	263488.1	847825.5	263300.4	855355.9	253752.0	849423.9	Agriculture
116	37	264651.5	849387.7	261523.8	854234.8	258321.3	848704.0	Agriculture
117	37	264402.6	847309.0	263939.3	856468.6	254840.0	850003.1	Agriculture
118	37	260620.1	851773.9	262375.8	856345.8	257254.7	850861.7	Agriculture
119	37	259874.5	850706.7	265325.4	860857.5	257272.2	850171.9	Agriculture
120	37	259603.1	852805.7	264905.4	853060.7	259961.2	852885.1	Agriculture
121	37	260184.2	850950.3	262319.9	856227.0	259059.6	847224.5	Agriculture
122	37	257496.4	851169.9	262680.7	851241.6	259605.0	853374.1	Agriculture
123	37	256281.5	849379.0	262234.0	851327.3	258555.0	853048.6	Agriculture
124	37	253682.2	850025.2	261461.4	851213.7	262126.4	854640.3	Agriculture

125	37	259459.0	847741.1	261519.5	851619.4	264399.6	845060.5	Agriculture
126	37	262483.6	849698.4	264575.9	849402.2	261855.4	854950.0	Agriculture
127	37	262578.7	849333.5	264242.3	847855.1	263362.2	854179.9	Agriculture
128	37	262839.5	848918.0	263685.5	847813.6	264800.6	853850.5	Agriculture
129	37	263225.6	848345.7	264968.1	846836.2	264463.6	853759.3	Agriculture
130	37	263692.5	847533.8	264368.6	845916.4	263394.9	853215.0	Agriculture
131	37	263716.7	847139.1	263727.4	844756.8	264306.8	853089.7	Agriculture
132	37	264137.2	846826.1	260379.0	844542.4	263202.1	852624.0	Agriculture
133	37	259786.9	852416.9	261220.9	846266.8	262436.6	852481.7	Agriculture
134	37	259202.2	851934.6	260784.5	846900.7	262448.1	852129.4	Agriculture
135	37	259873.2	851235.7	260402.2	846681.7	264902.6	852407.0	Agriculture
136	37	259014.9	850444.2	263268.5	847370.9	264568.5	851563.3	Agriculture
137	37	258888.8	849849.0	262661.2	846705.7	264851.1	851357.2	Agriculture
138	37	259128.1	849539.4	262098.2	846491.5	264463.7	851133.3	Agriculture
139	37	257533.1	851186.6	260355.4	847384.3	264204.7	851203.0	Agriculture
140	37	256748.2	849889.9	258697.1	850884.5	264428.8	850774.9	Agriculture
141	37	265677.9	846861.5	264705.3	847425.0	0	0	Waterbody
142	37	265769.2	846928.0	264730.6	847417.4	0	0	Waterbody
143	37	265689.1	847021.9	264702.7	847392.0	0	0	Waterbody
144	37	265614.5	846998.4	264673.0	847414.1	0	0	Waterbody
145	37	265602.2	847097.0	264693.6	847480.7	0	0	Waterbody
146	37	265529.6	847089.7	265974.6	847704.0	0	0	Waterbody
147	37	265423.7	847102.8	265049.8	847211.1	0	0	Waterbody
148	37	265417.4	847209.8	264979.2	847410.3	0	0	Waterbody
149	37	265331.4	847208.9	264960.4	847363.7	0	0	Waterbody
150	37	266075.5	847745.0	265095.4	847413.5	0	0	Waterbody
151	37	265748.5	847217.2	264725.2	847458.1	0	0	Waterbody
152	37	265006.4	847167.5	265202.8	847362.4	0	0	Waterbody
153	37	265325.2	848185.1	265004.4	847258.0	0	0	Waterbody
154	37	265004.6	847964.0	265247.3	847331.2	0	0	Waterbody
155	37	264984.2	847378.6	265375.2	847218.2	0	0	Waterbody
156	37	264945.6	847810.9	265417.5	847194.2	0	0	Waterbody
157	37	264909.3	848180.1	265452.5	847154.5	0	0	Waterbody
158	37	264827.9	847368.8	265454.3	847193.3	0	0	Waterbody
159	37	264754.5	847468.8	265408.9	847150.4	0	0	Waterbody
160	37	264683.2	847497.3	265384.1	847263.5	0	0	Waterbody
161	37	264684.4	847416.2	265599.9	847129.4	0	0	Waterbody
162	37	264623.6	848260.0	265470.5	847126.0	0	0	Waterbody
163	37	264241.9	847204.5	265537.7	847092.7	0	0	Waterbody
164	37	264752.0	847046.0	265503.2	847210.8	0	0	Waterbody
165	37	264222.8	846942.8	265460.6	847078.5	0	0	Waterbody
166	37	264603.8	847375.4	265379.6	847061.8	0	0	Waterbody
167	37	264912.3	847333.5	265310.3	847108.8	0	0	Waterbody

168	37	265101.5	847347.6	265279.2	847168.3	0	0	Waterbody
169	37	265368.3	847242.7	265202.0	847136.9	0	0	Waterbody
170	37	265523.2	847146.3	265560.8	847159.8	0	0	Waterbody
171	37	265697.8	847010.2	265585.2	847066.3	0	0	Waterbody
172	37	265549.4	847127.1	265808.8	847094.9	0	0	Waterbody
173	37	263967.2	847146.1	265606.6	847197.1	0	0	Waterbody
174	37	264170.8	847270.4	265645.5	846994.8	0	0	Waterbody
175	37	263805.0	846910.6	265634.1	846927.6	0	0	Waterbody
176	37	259568.8	848648.8	260638.9	848634.3	265607.4	846993.1	Wetland
177	37	260011.1	848044.7	265526.7	847028.8	265493.4	847139.4	Wetland
178	37	263727.1	846899.2	259502.5	848551.2	265560.0	847212.9	Wetland
179	37	263530.8	846799.5	259094.3	848552.4	265360.5	847266.7	Wetland
180	37	263334.6	846425.1	259912.1	848331.4	265172.3	847372.2	Wetland
181	37	263212.9	846356.9	260021.4	848116.4	264939.5	847397.0	Wetland
182	37	263021.4	846322.6	264208.8	847323.5	264642.6	847398.6	Wetland
183	37	263364.7	846558.3	258818.5	848512.5	264334.0	847256.6	Wetland
184	37	262794.7	846294.6	260146.8	849259.6	264091.0	847212.6	Wetland
185	37	263000.6	846306.0	260118.8	847855.0	263960.8	847008.7	Wetland
186	37	262396.2	846172.4	260375.0	847436.4	263810.7	847005.5	Wetland
187	37	262154.2	846060.3	264433.4	847326.5	264009.2	847188.1	Wetland
188	37	262325.2	846363.5	260826.0	847103.5	263554.9	846826.0	Wetland
189	37	261266.7	846784.4	261662.2	846261.5	263421.7	846668.0	Wetland
190	37	261391.8	846645.4	262008.7	845968.7	263048.0	846327.6	Wetland
191	37	261509.2	846464.9	261985.2	846131.4	262824.2	846154.3	Wetland
192	37	261606.9	846321.7	262405.0	846009.9	262650.2	846226.0	Wetland
193	37	261490.4	846164.2	262372.5	846066.4	262041.4	846101.2	Wetland
194	37	261736.8	846184.3	263935.8	846945.9	262360.9	846199.9	Wetland
195	37	261792.5	846131.1	264495.0	847228.8	262183.7	846083.0	Wetland
196	37	262001.0	846266.9	263789.8	846843.8	261975.9	846456.2	Wetland
197	37	261993.9	846002.5	263727.1	846825.3	261756.0	846182.3	Wetland
198	37	262193.3	846118.7	263874.0	846883.4	261562.2	846281.0	Wetland
199	37	262551.7	846138.5	263679.7	846882.9	260977.4	846966.7	Wetland
200	37	261362.2	846127.1	263682.2	846951.6	261198.7	846869.2	Wetland
201	37	260928.7	846995.8	263844.6	846981.6	261302.2	846811.8	Wetland
202	37	260352.2	847498.1	260821.0	847148.4	261385.5	846686.5	Wetland
203	37	260881.9	847081.0	260633.7	847289.4	260637.0	847303.2	Wetland
204	37	260752.3	847277.0	264750.3	847399.2	260294.0	847581.2	Wetland
205	37	260795.7	847163.0	265688.1	846945.9	259983.2	848309.9	Wetland
206	37	260552.2	847386.4	261699.3	849587.8	258862.5	848648.3	Wetland
207	37	260278.2	847431.6	259983.6	848046.2	258975.1	848671.3	Wetland
208	37	259607.8	848680.0	259939.3	848258.5	259924.0	848399.7	Wetland
209	37	259400.8	848620.2	258729.4	848606.1	260286.8	847467.4	Wetland
210	37	259107.5	848574.1	258912.7	848624.9	260951.8	846931.7	Wetland

Appendix II - LULC Classification Accuracy Assessment Report in 1987

		Ground truth data								
	Class name	FC	SET	SH	AG	WB	WE	Row Total	User accuracy	KC for each Category
Classified Image	FC	30	0	1	0	0	0	31	96.77%	0.9613
	SET	0	25	1	0	0	0	26	96.15%	0.9538
	SH	3	8	29	3	4	0	47	61.70%	0.5404
	AG	1	2	1	32	3	1	40	80.00%	0.7600
	WB	1	0	0	0	22	0	23	95.65%	0.9478
	WE	0	0	3	0	6	34	43	79.07%	0.7488
	Column Total	35	35	35	35	35	35	210		
	Producers Accuracy	85.71 %	71.43 %	82.86 %	91.43 %	62.86 %	97.14 %			
	Overall Accuracy								81.90%	
	(K^)									0.7829

Appendix III - LULC Classification Accuracy Assessment Report in 2003

		Ground truth data								
	Class name	FC	SET	SH	AG	WB	WE	Row Total	User accuracy	KC for each Category
Classified Image	FC	34	0	1	0	1	0	36	94.44%	0.9333
	SET	0	33	1	1	0	2	37	89.19%	0.8703
	SH	1	0	29	0	0	0	30	96.67%	0.9600
	AG	0	2	3	32	4	2	43	74.42%	0.6930
	WB	0	0	0	0	18	1	19	94.74%	0.9368
	WE	0	0	1	2	12	30	45	66.67%	0.6000
	Column Total	35	35	35	35	35	35	210		
	Producers Accuracy	97.14 %	94.29 %	82.86 %	91.43 %	51.43 %	85.71 %			
	Overall Accuracy								83.81%	
	(K^)									0.8057

Appendix IV - LULC Classification Accuracy Assessment Report in 2019

		Ground truth data								
Classified Image	Class name	FC	SET	SH	AG	WB	WE	Row Total	User accuracy	KC for each Category
	FC	32	0	0	0	0	1	33	96.97%	0.9621
	SET	0	31	0	0	0	1	32	96.88%	0.9609
	SH	3	0	30	0	0	0	33	90.91%	0.8864
	AG	0	2	4	32	0	2	40	80.00%	0.7500
	WB	0	0	0	0	0	0	0	--------	0.0000
	WE	0	2	1	3	0	31	37	83.78%	0.7973
	Column Total	35	35	35	35	0	35	180		
	Producers Accuracy	91.43 %	88.57 %	85.71 %	91.43 %	-----	88.57 %			
	Overall Accuracy								89.14%	
	(K^)									0.8643

Appendix V – Meteorological data

Parameter – Rainfall(mm)

Year	Jan.	Feb.	Mar.	Apr.	May.	Jun.	Jul.	Aug.	Sep.	Oct.	Nov.	Dec.
1987	17.78	129.86	312.74	320.6	553.19	392.87	257.42	216.59	273.84	213.88	64.06	30.64
1988	39.35	135.43	53.46	312.46	265.97	187.18	253.65	347.82	371.68	369.08	37.94	24.42
1989	49.14	105.74	231.67	270.48	206.17	283.01	395.26	246.72	252.78	197.53	87.45	188.33
1990	37.17	172.93	150.88	264.3	160.92	202.81	271.44	365.56	223.22	149.02	59	34.81
1991	59.1	81.06	138.67	238.3	349.42	212.78	254.15	202.9	177.95	97.76	36.47	75.94
1992	50.77	106.52	102.09	197.36	294.7	321.25	221.27	297.18	159.67	227.48	101.57	64.92
1993	96.45	77.34	106.59	295	385.7	389.87	277.03	304.94	131.87	272.9	45.72	9.67
1994	1.84	29.96	159.68	335.69	348.24	261.38	311.02	248.36	232.18	176.34	120.37	19.4
1995	9.86	66.71	164.29	321.86	276.91	293.98	227.18	221.03	285.68	201.11	69.71	105.55
1996	86.18	55.13	296.61	318.86	402.55	385.83	395.77	361.69	348.46	188.01	82.29	14.2
1997	34.91	6.18	97.76	430.76	322.74	312.08	197.4	211.63	170.65	504.42	270.26	97.57
1998	140.93	88.78	88.61	128.29	287.27	330.3	312.3	226.84	231.27	364.1	110.3	3.06
1999	36.05	6.79	98.1	173.24	257.77	182.74	220.29	155.1	128.1	296.11	23.56	18.93
2000	2.91	3.54	18.25	197.01	183.54	150.15	90.01	134.84	130.25	191.09	56.38	34.12
2001	36.83	26.4	126.62	221.45	210.53	170.08	86.4	108.66	100.69	145.27	56.81	13.9
2002	69.13	10.73	163.8	170.96	178.15	171	78.96	85.89	131.51	131.25	35.71	91.44
2003	15.13	22.98	135.51	131.38	92.78	130.7	70.46	144.58	79.14	39.15	71.3	78.05
2004	35.99	24.82	36.4	249.07	100.32	75.61	100.7	108.4	132.3	93.83	138.64	81.13
2005	33.89	22.35	133.56	235.51	302.03	80.8	125.13	84.06	125.59	101.59	42.28	0.27
2006	19.43	64.66	196.02	219.57	321.48	188.32	281.19	245.56	239.13	268.46	127.1	105.55
2007	60.9	81.96	132.31	253.97	343.72	215.23	265.65	274.49	265.56	143.92	84.34	11.51
2008	40.59	18.62	66.47	322.29	168.82	149.67	173.82	180.07	191.25	228.82	150.58	14.48
2009	59.42	28.29	100.79	290.35	154.18	104.19	149.42	178.91	227.7	279.21	39.82	131.28

2010	33.68	69.73	159.4	234.35	376.61	304.94	219.27	192.6	228.71	162.11	76.67	33.4
2011	26.29	11.12	80.9	200.57	268.04	164.37	102.32	95.9	116.12	117.79	189.53	14.6
2012	1.65	7.38	34.67	275.19	229.48	126.38	178.43	330.49	271.33	155.82	87.19	74.62
2013	31.67	14.83	160.89	336.61	457.61	275.49	235.9	223.59	182.7	235.22	183.85	10.37
2014	5.38	52.44	145.92	345.04	505.07	250.22	201.05	240.29	318.13	300.48	120.62	51.15
2015	1.45	20.77	60.14	111.54	218.05	250.77	206.76	137.1	83.13	191.94	75.88	85.87
2016	32.41	23.55	99.58	273.04	303.71	161.45	179.46	348.85	225.29	116.37	41.11	14.06
2017	2.48	95.57	81.39	136.55	278.49	169.36	217.78	176.43	250.36	148.6	52.62	1.57
2018	0.22	3.76	2.25	7.44	8.61	6.48	2.55	4.48	2.01	3.33	3.46	0.55
2019	0.01	1.14	2.6	7.52	5.07	7.2	5.73	7.77	9.57	6.55	3.69	2.15

Year	Jan.	Feb.	Mar.	Apr.	May.	Jun.	Jul.	Aug.	Sep.	Oct.	Nov.	Dec.
1987	12.61	14.2	15.26	15.01	15.23	14.69	14.24	14.15	14.85	14.51	12.05	11.95
1988	13.84	14.79	15.9	15.84	15.3	14.7	13.79	14.34	14.48	13.95	10.94	10.58
1989	11.84	13.17	15.27	14.97	14.86	14.28	14.11	13.89	14.15	13.38	13.26	14.24
1990	12.57	14.88	14.96	15.34	15.87	14.62	13.8	14.23	14.57	12.98	11.97	11.44
1991	13.84	15.03	15.72	15.49	15.66	15.15	13.96	14.06	13.98	12.74	11.83	12.16
1992	13.65	14.65	15.66	15.93	15.5	14.77	14.01	13.81	13.82	14.01	12.12	13.36
1993	13.22	13.86	14.56	15.62	15.25	14.59	13.78	13.92	13.94	13.9	12.22	11.91
1994	12.26	14.77	15.85	16.06	15.33	14.49	13.75	13.92	14.41	12.89	12.51	11.76
1995	12.51	14.85	15.65	16.26	15.36	15.01	13.98	14.1	14.42	13.9	12.15	13.36
1996	13.73	14.44	15.77	15.72	15.05	14.77	14.07	13.98	14.7	13.64	11.98	10.92
1997	13.89	12.92	16.69	15.63	15.14	15.1	14.28	14.5	14.81	14.68	14.38	14.08
1998	14.5	15.09	16.32	16.82	16.17	14.95	14.33	14.34	14.48	14.58	11.25	10.22
1999	12.47	13.67	15.66	16.19	15.08	14.32	13.6	13.99	14.1	13.88	11	11.55
2000	11.82	14.54	16.85	15.46	15.4	14.55	13.99	13.95	14.59	14.28	12.85	12.82
2001	14.09	15.49	15.5	15.91	15.71	14.26	14.14	13.82	14.8	14.42	12.12	14.23
2002	14.05	15.35	16.24	15.5	15.86	14.76	14.58	14.53	14.89	14.01	13.47	14.63
2003	14.24	17	16.24	15.62	16.09	14.97	14.48	14.14	14.94	14.71	14.39	12.7
2004	15.43	15.33	16.75	16.11	15.69	14.85	14.21	14.56	14.78	13.38	13.64	14.13
2005	13.73	15.82	16.24	16.47	15.48	14.93	14.11	14.53	14.84	13.91	12.35	11.29
2006	14.53	15.55	15.87	15.22	15.63	14.74	14.3	14.21	14.45	14.49	12.2	12.87
2007	13.1	14.67	14.92	15.43	15.67	14.84	13.96	14.22	14.5	12.71	11.26	9.77
2008	12.9	14.19	15.8	14.99	15.33	14.14	13.91	14.29	14.42	13.4	11.61	10.97
2009	12.62	14.54	16.33	15.82	15.33	15.28	14.26	14.51	14.91	14.06	11.67	13.9
2010	13.35	15.63	15.05	16.14	16.34	15.27	14.32	14.27	14.65	13.75	11.56	11.7
2011	12.82	14.18	15.43	15.67	15.72	14.86	14.5	14.21	14.65	12.99	13.51	11.76
2012	13.51	14.22	16.62	15.79	15.69	14.89	14.13	14.22	14.67	13.18	12.74	12.47
2013	13.46	14.93	16.27	15.6	15.6	14.7	13.93	13.94	14.56	13.54	13.06	10.94
2014	13.46	14.83	16.02	15.7	15.95	15.18	14.59	14.32	14.7	13.82	13.1	11.04
2015	11.23	14.6	16.11	16.06	15.88	15.23	14.88	14.73	15.24	14.88	13.29	13.94
2016	15.52	15.7	17.35	16.47	15.88	14.97	14.35	14.18	14.56	14.3	12.34	11
2017	10.2	15.31	16.23	16.77	16.09	15.4	14.49	14.6	14.85	14.64	12.36	10.05

2018	12.9	15.26	15.24	15.53	15.81	14.56	14.2	14.18	14.79	14.51	13.89	14.04
2019	13.36	16.83	17.23	16.53	16.38	15.25	14.56	14.62	14.9	14.06	14.15	13.51

Parameter – Minimum temperature (°C)

Parameter – Maximum temperature (°C)

Year	Jan.	Feb.	Mar.	Apr.	May.	Jun.	Jul.	Aug.	Sep.	Oct.	Nov.	Dec.
1987	25.38	26.42	24.06	23.86	21.96	21.57	21.66	21.76	22.32	22.3	22.7	23.63
1988	25.74	26	28.65	25.93	23.24	21.64	20.96	21.28	21.28	21.82	22.61	23.5
1989	24.5	25.17	25	23.19	22.97	21.4	21.1	21.34	21.36	22.08	22.83	22.51
1990	23.48	24.08	23.98	23.54	23.21	21.25	21.05	21.33	21.92	22.45	23.12	24.53
1991	25.78	26.49	26.36	24.4	23.72	22.52	21.16	21.39	21.91	22.51	23.32	23.73
1992	25.4	24.89	27.48	26.17	23.28	21.61	20.92	20.8	21.62	21.49	22.3	23.17
1993	23.04	24.44	26.32	23.59	22.66	21.22	20.74	21.51	22.01	22.01	22.94	23.98
1994	27.02	28.63	27.2	24.81	23.12	20.91	20.52	21.17	22.02	22.63	23	23.89
1995	26.39	26.58	26.51	24.34	22.92	22.45	20.72	21.56	21.76	22.1	22.88	23.03
1996	23.58	26.25	25.03	23.24	22.45	21.19	20.6	21.29	21.52	22.2	22.44	23.19
1997	25.03	29.16	29.13	23.18	22.58	21.86	21.19	21.79	22.46	21.64	22.66	23.46
1998	23.62	24.3	25.72	26.29	23.23	22.19	20.67	21.45	22.13	21.82	22.65	23.27
1999	25.31	30.16	27.69	25.59	22.38	21.82	20.65	21.76	22.39	21.45	22.63	24.33
2000	28.07	30.42	31.48	25.46	22.96	22.39	22.3	22.8	23.2	22.48	23.84	25.65
2001	25.67	28.88	26.93	24.93	22.9	21.42	22.38	22.05	23.01	23.4	24.37	26.67
2002	25.77	30.14	26.7	25.4	24.08	22.02	23.53	23.45	24.26	24.1	26.11	25.79
2003	26.97	30.31	28.59	27.01	27.59	23.16	23.15	22.66	24.08	27.33	27.94	26.65
2004	28.24	29.57	30.7	24.58	24.67	22.51	23.26	23.26	23.72	24.63	25.08	26.24
2005	27.08	31.45	27.71	27.2	23.14	22.26	21.58	23.08	23.19	24.01	25.61	28.75
2006	29.77	29.31	26.34	24.33	23.24	21.87	21.22	21.53	21.91	22.47	22.99	23.17
2007	23.9	25.07	26.8	24.73	23.38	21.67	21.55	21.23	21.7	22.62	22.92	24.05
2008	26.88	28.62	30.63	24.17	22.8	21.67	21.45	21.8	22.08	22.43	22.49	23.61
2009	25.02	28.07	28.6	24.52	24.25	23.19	22.19	22.64	22.86	22.53	23.53	23.12
2010	24.58	25.65	26.53	24.4	22.76	22.04	21.35	21.69	21.74	22.94	22.97	23.18
2011	25.07	29.25	27.94	26.06	22.88	21.73	21.96	21.9	22.31	23.93	22.87	24.76
2012	28.19	31.24	30.24	25.03	23.47	21.79	21.4	21.7	21.6	23	23.02	23.48
2013	25.29	28.62	27.29	24.53	22.36	21.24	20.96	21.05	21.86	22.11	22.76	23.05
2014	24.9	26.29	27.22	23.48	22.71	22.17	21.59	21.38	21.59	22.08	22.86	22.9
2015	24.92	28.29	29.73	27.8	23.62	22.37	22.03	22.73	23.67	23.63	23.71	24.37
2016	26.07	29.07	29.44	24.49	22.58	22.22	21.73	21.77	22.32	22.6	23.14	24.7
2017	28.18	27.82	28.16	28.87	23	22.46	21.75	22.17	22.05	23.11	22.87	24.95
2018	27.2	27.96	27.59	24.38	23.07	21.16	21.67	22.11	23.73	24.03	24.45	27.25
2019	30.26	30.18	29.71	25.51	24.39	22.11	21.98	22.07	22.26	23.07	22.99	23.79